

BYG·DTU

DANMARKS
TEKNISKE
UNIVERSITET



Miriam Lykke Mølgaard

Wettability and capillary
measurement on Hillerslev outcrop
chalk

Rapport
BYG·DTU
R-132
2006
ISSN 1601-2917
ISBN 87-7877-203-6

Wettability and Capillary Pressure Measurements on Hillerslev Outcrop Chalk

Miriam M. Lykke

Ph.D. Thesis

Department of Civil Engineering
Technical University of Denmark

2005

Wettability and Capillary Pressure Measurements on Hillerslev Outcrop
Chalk

Copyright (c), Miriam M. Lykke, 2005

Printed by

Department of Civil Engineering

Technical University of Denmark

Preface

This report is part of the written documentation of the Ph.D. project: "Displacement of Oil by Waterflooding in Fractured Chalk". The Ph.D. project was coordinated with and partly financed by a Danish Energy Research Programme (EFP) project 2000. The title of this project is "Displacement and Deformation Processes in Fractured Reservoir Chalk" (Christensen 2003), and the main objective was to quantify the displacement processes in fractured reservoir chalk. The research partners were: Danish Geotechnical Institute (GEO), Geological Survey of Denmark and Greenland (GEUS), Department of Environment and Resources (ER), DTU and Department of Civil Engineering (BYG•DTU), DTU. The industrial partners were: BP Norway and Mærsk Olie og Gas AS.

This report documents the laboratory studies of two-phase flow properties such as wettability characteristics and capillary pressure curves for Hillerslev outcrop chalk used in the integrated research project.

I am grateful to Rogaland Research, Norway for letting me perform wettability and capillary pressure measurements on three small Hillerslev outcrop chalk specimens at their premises. I wish to thank Research Engineer Jan Erik Iversen, Rogaland Research and Engineer Egil Boye Petersen, working at Rogaland Research when the measurements were initiated, for help and supervision during the measurements.

Furthermore, I wish to thank Professor Rasmus Risnes, Professor Tor Austad, Post Doctor Dag C. Standnes and Professor Svein Skjæveland at Stavanger College, Norway for fruitful discussions about wettability and capillary pressure. Stavanger College, Norway is acknowledged for a pleasant stay there.

Lyngby, April 2005

Miriam M. Lykke

Abstract

Measurement of wettability and subsequent establishment of capillary pressure curves was carried out for three small Hillerslev outcrop chalk specimens. This was done by utilizing Amott cups and an automated Beckman centrifuge at Rogaland Research, Stavanger, Norway. The dimensions of the specimens were $D = 38$ mm and $H = 50$ mm. The fluids used were synthetic Valhall formation water and the laboratory oil Isopar-L. Two of the specimens tested were originally water-wet, while the wettability of a single specimen was altered to a homogenous neutral to slightly oil-wet state. However, the wettability alteration affected the chalk, and the specimen broke in one end. Consequently, a new diameter and height were obtained, i.e. $D = 37.9$ mm and $H = 36.2$ mm.

The modified U. S. Bureau of Mines (USBM) method was used to obtain both the Amott-Harvey and the USBM wettability indices. The method consists of five steps: (1) initial oil drive, (2) spontaneous imbibition of water, (3) water drive, (4) spontaneous imbibition of oil, and (5) oil drive.

It was concluded that Hillerslev outcrop chalk is strongly water-wet and that it can be altered towards a homogeneous neutral to slightly oil-wet state using crude oil added with 1 weight% Dodekane acid. It was found that the USBM wettability index cannot be obtained for strongly water-wet Hillerslev outcrop chalk.

Water-oil capillary pressure curves were established for the specimens based on the measurements during the modified USBM method. However, due to centrifuge limitations, the capillary pressure curves were not fully completed. Further, fractures were induced during centrifuging. It is evaluated that the obtained capillary pressure curves are not fully representative for the specimens. However, a good estimate of the residual oil saturation S_{orw} was obtained, especially for the strongly water-wet specimens.

Based on the fact that the capillary pressure curves were not fully completed due to centrifuge limitations, and that fractures were induced in the specimens even at these lower centrifuge speeds, it is evaluated that capillary pressure curves cannot be obtained in the centrifuge for Hillerslev chalk.

Table of Contents

1	Introduction	1
2	Wettability and Capillary Pressure Measurement	3
2.1	Measuring Methods for Wettability	3
2.2	Establishing Capillary Pressure Curves	9
3	Description of the Laboratory Tests	17
3.1	Hillerslev Chalk Specimens and Fluids	17
3.2	Preparation of the Specimens	18
3.3	Test Procedure	22
4	Laboratory Test Results	25
4.1	Wettability Determination	25
4.2	Capillary Pressure Curves	30
5	Conclusions	37
	Bibliography	39
A	Discrete Solutions for End-Face Saturation	41
B	Gravity and Radial Effects on Capillary Pressure	43
C	Laboratory Journal	47
D	Description of Specimens 1, 2 and 3	49
E	Absolute Water Permeability for Specimens 1 and 2	51
F	Production Curves for the Centrifuge Tests	53

Chapter 1

Introduction

This report provides information on wettability and capillary pressure measurements for Hillerslev outcrop chalk used for large-scale waterflooding tests performed in the Ph.D. project. Hillerslev outcrop chalk was chosen for the tests as this chalk is available for sampling of large specimens and it is highly fractured. Further, the chalk can be regarded as a close analogue to the oil-producing Tor formation of the Valhall field. Like Hillerslev chalk, the Valhall Tor formation is of Late Maastrichtian age and is heavily fractured. The chalk from the Hillerslev quarry and the Valhall Tor formation has the same degree of low cementation, low hardness, high porosity and low permeability (Krogsbøll et al. 1997). The fracturing of the Valhall Tor formation and the Hillerslev chalk are considered comparable due to similar structural development (Ali & Alcock 1992). Prior to testing, Hillerslev outcrop chalk was considered water-wet whereas the Valhall Tor formation was reported neutral to slightly oil-wet (Andersen 1995) or neutral to slightly water-wet (Eltvik et al. 1990).

The success of waterflooding depends on the capillary pressure curves for the material, i.e. the relationship between saturation and capillary pressure. Wettability affects both capillary pressure and waterflooding. It is thus important to obtain knowledge about wettability and capillary pressure properties for Hillerslev outcrop chalk in order to obtain a better understanding of the displacement processes in oil-saturated Hillerslev outcrop chalk during waterflooding.

Wettability and capillary pressure measurements were performed on three small ($D = 38$ mm, $H = 50$ mm) Hillerslev outcrop chalk specimens at Rogaland Research in Stavanger, Norway. The aims of these tests were to:

- Measure the wettability of Hillerslev outcrop chalk (the degree of water-wetness)
- Establish capillary pressure curves for Hillerslev outcrop chalk
- Alter the wettability of a small Hillerslev outcrop chalk specimen towards the wettability of the Valhall Tor formation
 - To learn how to alter the wettability
 - To establish capillary pressure curves for a small wettability-altered specimen

Introduction

- To obtain knowledge of the effect of the wettability of Hillerslev outcrop chalk on capillary pressure measurements
- To be able to alter the wettability of a large specimen in order to perform waterflooding test on a specimen as close an analogue to the Valhall Tor formation as possible
 - * To obtain knowledge of the effect of the wettability of Hillerslev outcrop chalk on waterflooding

The specimens were prepared at Stavanger College, Norway. The tests were planned and carried out by the author with help and supervision from Research Engineer Jan Erik Iversen, Rogaland Research, and Engineer Egil Boye Petersen, earlier working at Rogaland Research. The data processing, evaluation and reporting was carried out by the author.

Chapter 2

Wettability and Capillary Pressure Measurement

2.1 Measuring Methods for Wettability

Wettability can be measured in the laboratory. Three quantitative methods are generally used: (1) contact angle measurement, (2) the Amott test, and (3) the U. S. Bureau of Mines (USBM) test. The contact-angle measures the wettability of a specific surface, while the Amott and USBM tests measure the average wettability of a specimen. The two latter methods are also used in a combined test referred to as the modified USBM test.

Contact Angle Measurement

Contact angles can be measured by submerging two smooth parallel mineral plates in water and then introduce a drop of oil between the plates. When the plates are moved relative to each other, a contact angle is formed. The maximum angle is obtained by pushing the fluid over the surface, while the minimum is obtained by pushing the fluid back. The maximum and the minimum angles measured through the same fluid are referred to as the advancing contact angle and the receding contact angle, respectively.

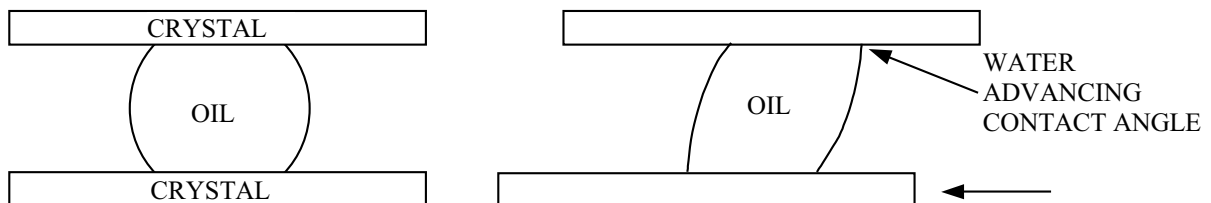


Figure 2.1 *Set-up for contact angle measurement.*

Morrow (Morrow 1990) states that water-advancing contact angles are reported as defining wettability because these are considered relevant to waterflooding. A range of

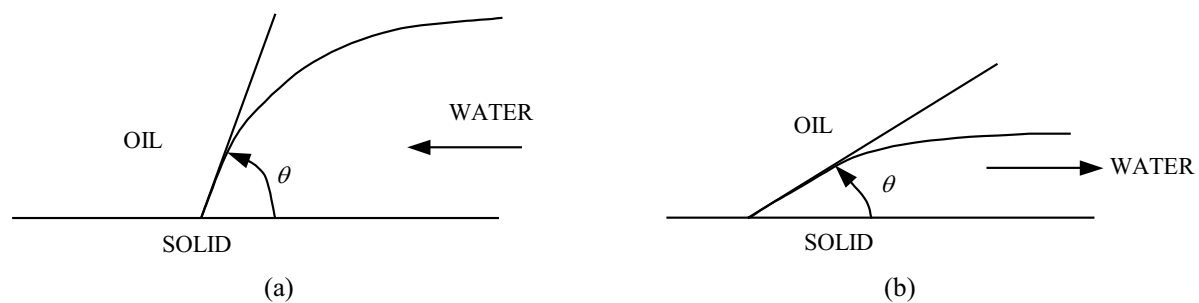


Figure 2.2 *Hysteresis in contact angle in a water-wet porous medium (a) increase in the wetting fluid (imbibition) and (b) decrease in the wetting fluid (drainage).*

contact angles will be measured in most systems, however, with relatively reproducible maximum and minimum values.

The difference between the two angles is the contact-angle hysteresis, which can be greater than 60° . There appears to be three causes of contact-angle hysteresis: surface roughness, surface heterogeneity and surface immobility on a macro-molecular scale. Contact angle hysteresis is one factor causing hysteresis between capillary pressures measured with increasing vs. decreasing wetting fluid saturations (Anderson 1986a). The measured value of the contact angle may also depend strongly on the time of exposure of the solid to both fluids, as alteration of the surface wettability can occur. The concept of explaining wettability based on the contact angle is not very useful, since it is based on a plane surface to measure from.

Amott Test

The Amott test combines spontaneous and forced imbibition to measure the average wettability of a specimen. The method is based on the fact that the wetting fluid will generally imbibe spontaneously into the specimen and displace the nonwetting one. The ratio of spontaneous to forced imbibition is used to reduce the influence of other factors such as relative permeability, viscosity and the initial saturation of the specimen. Based on the test, the Amott-Harvey wettability index WI can be calculated. The index compares the imbibition potential of water and oil, and varies from +1 for strongly water-wet specimens to -1 for strongly oil-wet specimens (Anderson 1986a).

In the first step of the Amott test, the specimen is centrifuged first in water and then in oil to reduce the specimen to the irreducible water saturation S_{wir} . Then it consists of the following four steps: (1) immerse the specimen in water, and measure the volume of oil displaced spontaneously, (2) centrifuge the specimen in water until the residual oil saturation S_{orw} is reached, and measure the amount of oil displaced under force, (3) immerse the specimen in oil, and measure the volume of water displaced spontaneously, and (4) centrifuge the specimen in oil until S_{wir} is reached, and measure the amount of water displaced under force. The specimen may be driven to S_{wir} and S_{orw} by flow rather than with a centrifuge.

The calculation of the Amott-Harvey index uses three wettability indices. The water-wetting index WWI is the displacement-by-water ratio, i.e. the ratio of the spontaneous

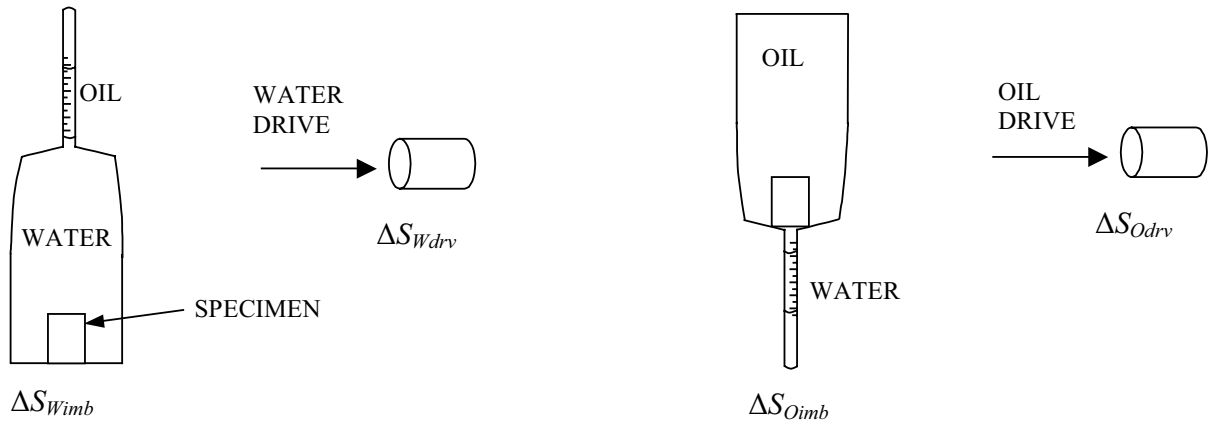


Figure 2.3 Set-up for measurement of the Amott-Harvey wettability index.

saturation change to the total saturation change and can be defined for spontaneous water imbibition ΔS_{Wimb} and driven water saturation change ΔS_{Wdrv} as (Andersen 1995):

$$WWI = \frac{\Delta S_{Wimb}}{(\Delta S_{Wimb} + \Delta S_{Wdrv})} \quad (2.1)$$

An oil-wetting index OWI is defined similarly for spontaneous oil imbibition, ΔS_{Oimb} and driven oil saturation change ΔS_{Odrv} , i.e. the displacement-by-oil ratio. In the Amott test, the displacement-by-water ratio is zero for neutrally and oil-wet specimens and approaches 1 as the water-wetness increases. Similarly, the displacement-by-oil ratio is zero for neutrally and water-wet specimens and approaches 1 as the oil-wetness increases.

The Amott-Harvey wettability index is the displacement-by-water ratio minus the displacement-by-oil ratio. This combines the two ratios into a single wettability index:

$$WI = WWI - OWI \quad (2.2)$$

USBM Test

The USBM test includes measurement of drainage and imbibition capillary pressure curves, usually by use of a centrifuge. The method compares the work necessary for one fluid to displace the other. Because of the favourable free-energy change, the work required for the wetting fluid to displace the nonwetting fluid from the specimen is less than the work required for the opposite displacement. It has been shown that the required work is proportional to the area under the capillary pressure curve. Based on the USBM test, the USBM wettability index can be calculated. This index is unbounded. Experimentally though, the index usually falls within -1 to +1. According to Man and Jing (Man & Jing 2000), the specimen is preferentially water-wet if the index is greater than zero. If the index is less than zero, the specimen is preferentially oil-wet. The specimen is neutral-wet if the index is approximately zero.

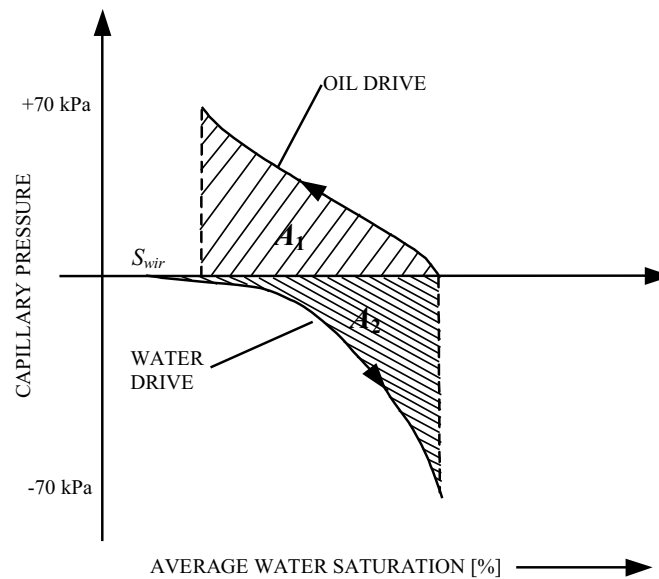


Figure 2.4 Schematic of wettability measurements by the USBM method for a mixed-wet system.

Before the USBM test, the specimen is prepared by centrifuging first in water and then in oil to S_{wir} . In the first step of the USBM test, the specimen is placed in water and centrifuged at incrementally increasing speeds. This step is known as the water drive because water displaces oil from the specimen. At each incremental speed, the average saturation of the specimen is calculated from the volume of expelled oil and the capillary pressure is calculated from the rotational acceleration (Section 2.2). In the second step, the specimen is placed in oil and centrifuged. During this oil drive, the capillary pressures and average saturations are calculated. Both the water drive and the oil drive are carried out until a capillary pressure of 70 kPa (10 psi) is reached. In each case (oil- and water drive), the curves are linearly extrapolated or truncated if the last pressure is not exactly 70 kPa. The USBM method uses the ratio of the areas under the two capillary pressure curves to calculate a wettability index (Anderson 1986a). In Figure 2.4, the schematic of the determination of the wettability index by the USBM test for a mixed-wet system is shown.

The USBM index is the log of the ratio of areas under the water and oil drive part of the capillary pressure curves for a capillary pressure between -70 kPa and 70 kPa:

$$USBM\ index = \ln(A_1/A_2) \quad (2.3)$$

where A_1 is the area under the oil drive curve, and A_2 is the area above the water drive curve.

Modified USBM Test

A modified USBM method exists which is a combined Amott and USBM test that allows for calculation of both the Amott-Harvey and the USBM wettability indices. There are two advantages of combining these tests. Firstly, the resolution of the USBM test is

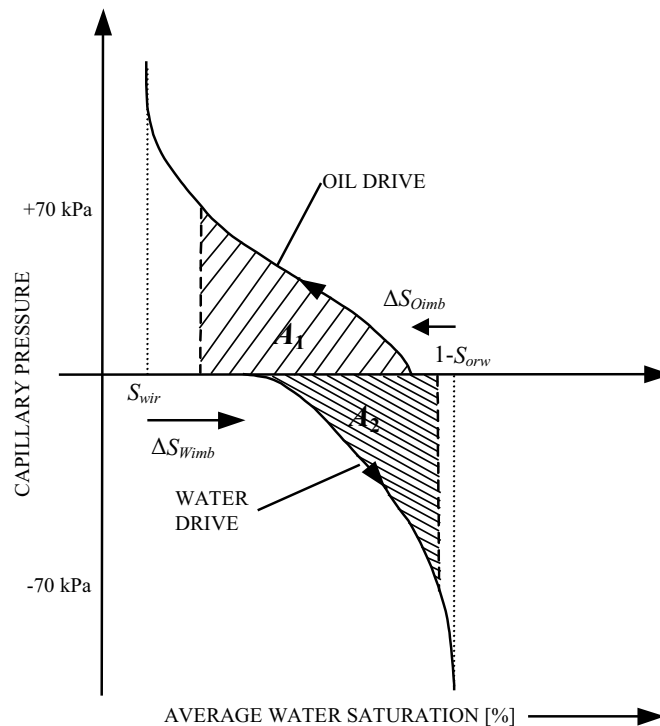


Figure 2.5 Schematic of wettability measurements by the modified USBM method for a mixed-wet system.

improved by accounting for the saturation changes that occur at zero capillary pressure, and secondly, the Amott-Harvey index is calculated as well. The procedure has five steps: (1) the specimen is prepared by centrifuging first in water and then in oil to S_{wir} , (2) spontaneous imbibition of water, (3) water drive, (4) spontaneous imbibition of oil, and (5) oil drive. In the second step, the specimen is immersed in water, and the volume of water that imbibes spontaneously is measured. During the water-drive, the average saturation of the specimen is determined from the volume of expelled oil at each incremental capillary pressure calculated from the rotational acceleration. At the end of the water-drive, the specimen is left at S_{orw} . In the fourth step, the specimen is immersed in oil, and the volume of oil that imbibes spontaneously is measured. The final step is the oil drive, where the specimen again is driven to S_{wir} (Anderson 1986a). A sketch of the wettability measurements established by the modified USBM method for a mixed-wet system is shown in Figure 2.5.

The areas under the water and oil drive curves are used to calculate the USBM index, while the Amott-Harvey index uses the volumes of spontaneous and total water and oil displacements.

The modified USBM method is best illustrated for a non-homogeneous wet system, but as the Amott-Harvey and the USBM wettability indices are a measure of the average wettability of a specimen, such indices are not very representative for specimens with non-homogeneous wettability.

For both the USBM test and the modified USBM method, the original USBM index is found from the area under the capillary pressure vs. average saturation curve. A modified

USBM index is found from the area under the capillary pressure vs. end-face saturation curve. In this report, the average saturation of the specimen is used for determination of the USBM index, i.e. the original USBM index is calculated. In contrast, the capillary pressure curves are based on the saturation at the end-face of the specimens, which is calculated from the average saturation (Section 2.2).

The USBM test appears to be superior to the Amott test, which is insensitive near neutral wettability. It is possible to have an Amott-Harvey wettability index of about zero either because the material imbibes neither water nor oil strongly, or because it imbibes quite a bit of both to the same degree. However, the USBM test cannot determine whether a system has homogeneous wettability or not, while the Amott test is sometimes sensitive. In some fractional- or mixed-wet systems, both water and oil imbibe spontaneously. The Amott test will have positive displacement-by-water and displacement-by-oil ratios, indicating that the system is non-homogeneously wetted. There are thus two advantages of the combined Amott and USBM test. It provides sensitivity near neutral wettability and will sometimes indicate if a system is non-homogeneously wetted (Anderson 1986a).

In Table 2.1 the approximate relationship between wettability, contact angle, and the USBM and Amott-Harvey wettability indices are included.

	Water-wet	Neutral-wet	Oil-wet
Contact angle			
Minimum	0°	60° to 75°	105° to 120°
Maximum	60° to 75°	105° to 120°	180°
USBM wettability index	W near 1	W near zero	W near -1
Amott test			
Displacement-by-water ratio	Positive	Zero	Zero
Displacement-by-oil ratio	Zero	Zero	Positive
Amott-Harvey wettability index	$0.3 \leq WI \leq 1.0$	$-0.3 < WI < 0.3$	$-1.0 \leq WI \leq -0.3$

Table 2.1 *Approximate relationship between wettability, contact angle, and the USBM and Amott-Harvey wettability indices (Anderson 1986a).*

According to Anderson (Anderson 1986a), a qualitative wettability measurement method is the imbibition method because it gives a quick but rough idea about the wettability. The imbibition method can be described as a modified form of the Amott test since the imbibition rates during the spontaneous imbibition measurements is also measured. In this test, the specimen is suspended in oil or water from an electronic balance by a small line. Weight change is monitored as a function of time as spontaneous imbibition occurs. The degree of wetness is indicated by the rate and volume of imbibition. The specimen is strongly water-wet if large volumes of water imbibe rapidly, while lower rates and smaller volumes imply a more weakly water-wet specimen. This is similar for imbibition of oil in an oil-wet specimen. If neither oil nor water imbibe spontaneously, the specimen is neutral-wet. Finally, some specimens will imbibe both water and oil spontaneously. These specimens have either fractional- or mixed-wettability. One problem with the imbibition method is that in addition to wettability, imbibition rates also depend on relative permeability, viscosity, IFT, pore structure, and initial saturation of the speci-

men. This dependence may be reduced by comparison of the measured imbibition rate with a reference rate measured when the specimen is strongly water-wet.

2.2 Establishing Capillary Pressure Curves

Capillary pressure measurements are essential for a complete characterization of an oil-bearing reservoir. Capillary pressure curves can be used for estimation of reserves, for reservoir evaluation or as input to reservoir simulation. Capillary pressure curves can be obtained in the laboratory by at least three different techniques. (1) The mercury injection method. As mercury is a nonwetting fluid for reservoir rock, drainage capillary pressure curves can be obtained. (2) The porous plate method. The specimen is placed on a diaphragm wet by the fluid to be displaced from the specimen. During increase in the displacing pressure, the corresponding saturation is determined. (3) The centrifuge method. Here, the pressure difference between the fluids results from the density difference.

Christoffersen (Christoffersen 1995) reports that the porous-plate method is considered the most accurate, whereas the mercury injection method and the centrifuge method are much faster to perform. An obvious disadvantage of the mercury injection method is that a different fluid system is used. The porous plate method directly measures the capillary pressure curve, while the centrifuge method is an indirect method and additional data processing is required to obtain a capillary pressure curve.

Earlier experimental work by Nørgaard et al. (Nørgaard et al. 1999) has shown that capillary pressure curves obtained by mercury injection lie significantly below a capillary pressure curve obtained by the centrifuge method on the same specimen of North Sea Chalk. The reason for this may lie in problems with scaling of the interfacial tension (IFT) and contact angle of the mercury liquid - mercury vapor system to the water-oil system (Anderson 1986*b*).

As mentioned, capillary pressure curves can be obtained by the centrifuge method, where the pressure difference between the fluids results from the density difference, as in the gravity-driven process in the field. The capillary pressure is not directly measured, but found from the centrifuge speed by assuming exact analogy of a centrifugal field and a gravitational field. First, centrifuge production data, i.e. corresponding values of centrifuge speed and produced volumes are measured. When the wettability of a specimen is known, these data can be transformed into capillary pressure curves.

The initial work on the centrifuge method was introduced in 1945 by Hassler and Brunner (Hassler & Brunner 1945). They introduced the theory and practice of using the centrifuge to create a pressure gradient within the specimen and presented an approximation for converting measured average saturation to end-face saturation for drainage curves. Szabo (Szabo 1974) extended the method to include imbibition curves. Over the years, various interpretation methods for improving the Hassler and Brunner derivation have been published. Forbes (Forbes 1994) concludes that the simple methods usually reduce the accuracy of the results, while the accurate ones usually require more time and must smooth, fit, or force the experimental data into a given analytical form.

The centrifuge method consists in measuring average fluid saturation versus capillary pressure P_c of a specimen at hydrostatic equilibrium during rotation at various angular

velocities ω , see Figure 2.6. The specimen is initially filled with a fluid and spun within a second fluid. Due to the rotation, the inner fluid is forced out of the specimen. The average saturation of a specimen can be determined at the different centrifuge speeds by collecting and measuring the fluid production.

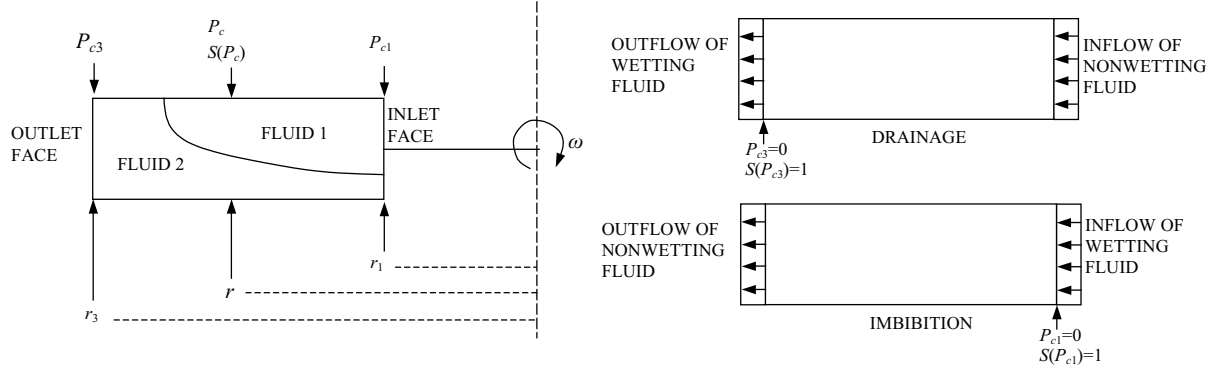


Figure 2.6 Schematic of the centrifuge method (Forbes 1994).

According to Hassler and Brunner (Hassler & Brunner 1945), at hydrostatic equilibrium, the capillary pressure at any position is equivalent to the difference in hydrostatic pressure between the two phases. Taking the linear variation of the centrifugal field with the distance from the axis of rotation into account, the capillary pressure P_c [Pa] for drainage is given by:

$$\int_{P_{wetting}}^{P_{nonwetting}} dP = \int_r^{r_3} \Delta\rho\omega^2 r dr \quad (2.4)$$

⇓

$$P_c = \frac{1}{2}\Delta\rho\omega^2(r_3^2 - r^2) \quad (2.5)$$

where r [m] is the radial distance from the axis of rotation, r_3 [m] is the radius to the center of the outlet face of the specimen, ω [rad/sec] is the angular velocity of the centrifuge and $\Delta\rho$ [kg/m³] is the density difference between the two phases defined as:

$$\Delta\rho = \rho_{wetting} - \rho_{nonwetting} \quad (2.6)$$

For drainage, it is assumed that the capillary pressure $P_c = 0$ at the outlet face (Figure 2.6), and the capillary pressure at the inlet face P_{c1} is calculated as:

$$P_{c1} = \frac{1}{2}\Delta\rho\omega^2(r_3^2 - r_1^2) \quad (2.7)$$

where r_1 [m] and r_3 [m] are the distances to the centers of the inlet and the outlet face of the specimen, respectively.

If the variation of the centrifugal field with the distance from the axis of rotation is taken into account, the average saturation for drainage of the specimen can be found from:

$$\bar{S} = \frac{1}{(r_3 - r_1)} \int_{r_1}^{r_3} S(r) dr \quad (2.8)$$

This can be rewritten into the fundamental equation for converting average wetting phase saturation for drainage into local average saturation (inlet face) formulated by Hassler and Brunner:

$$\bar{S}(P_{c1}) = \frac{1 + \sqrt{1 - B}}{2} \int_0^1 \frac{S(xP_{c1}) dx}{\sqrt{1 - Bx}} \quad (2.9)$$

where x is a dimensionless integration variable, and:

$$B = 1 - \left(\frac{r_1}{r_3}\right)^2 \quad 0 \leq B \leq 1 \quad (2.10)$$

For forced imbibition, the same equations are obtained when exchanging r_1 for r_3 (Forbes 1994). For imbibition, it is assumed that the capillary pressure $P_c = 0$ at the inlet face (Figure 2.6), and the capillary pressure at the outlet face P_{c3} is calculated as:

$$P_{c3} = \frac{1}{2} \Delta \rho \omega^2 (r_1^2 - r_3^2) \quad (2.11)$$

The fundamental equation for converting average wetting phase saturation for imbibition into average local saturation (outlet face) is given by:

$$\bar{S}(P_{c3}) = \frac{1 + \sqrt{1 - B}}{2} \int_0^1 \frac{S(xP_{c3}) dx}{\sqrt{1 - Bx}} \quad (2.12)$$

where:

$$B = 1 - \left(\frac{r_3}{r_1}\right)^2 \quad B < 0 \quad (2.13)$$

The essential problem that must be solved to obtain a capillary pressure curve is to relate P_c to its appropriate end-face saturation S . For both drainage and imbibition, the problem consists therefore in inverting the fundamental average saturation equations $\bar{S}(P_{c1})$ and $\bar{S}(P_{c3})$ to obtain $S(P_{c1})$ and $S(P_{c3})$, respectively.

For drainage, Hassler and Brunner proposed the approximate solution for calculating the end-face saturation from the measured average saturation:

$$S = S_{HB} = \bar{S} + P_c \frac{d\bar{S}}{dP_{c1}} \quad B = 0 \quad (2.14)$$

For imbibition P_{c1} is replaced by $-P_{c3}$. This solution is based on the assumption of a linear variation of P_c along the specimen. The solution has increasing errors outside the range of $r_1/r_3 \geq 0.7$. The solution rests on the assumption that the model is one-dimensional. Centrifugal acceleration and fluid flow are assumed to be parallel to the axis

of the core. According to Forbes (Forbes 1994), this solution is one of the worse solutions outside the range of $r_1/r_3 \geq 0.7$, but is still widely used in the oil industry.

Van Domselaar (Forbes 1994) proposed the following approximate solution for drainage:

$$S = S_D = \bar{S} + \frac{2\sqrt{1-B}}{1+\sqrt{1-B}} P_c \frac{d\bar{S}}{dP_{c1}} \quad (2.15)$$

For imbibition P_{c1} is replaced by $-P_{c3}$. As for the S_{HB} solution, the approximation to the correct $S(P_c)$ is accurate enough for $r_1/r_3 \geq 0.7$.

Forbes (Forbes 1994) proposed an accurate, rapid and simple method that allows for conversion of sparse and noisy experimental data without smoothing, fitting, averaging, or forcing data to a given form. Forbes believes this method to produce capillary pressure curves corresponding more closely to the centrifuge data than curves obtained from most other methods, and it is particularly simple for imbibition. The accurate approximate solution for drainage is given by:

$$S(P_c) \approx S_{\alpha\beta} = \left(1 - \frac{B}{2}\right) S_\alpha + \frac{B}{2} S_\beta \quad 0 \leq B \leq 1 \quad (2.16)$$

where:

$$S_\alpha(P_c) = \bar{S}(P_c) + \frac{P_c}{1+\alpha} \frac{d\bar{S}(P_c)}{dP_{c1}} \quad \alpha = \frac{1 - \sqrt{1-B}}{1 + 2\sqrt{1-B}} = \frac{r_3 - r_1}{r_3 + 2r_1} \quad (2.17)$$

$$S_\beta(P_c) = (1 + \beta) \int_0^1 x^\beta S_{HB}(xP_c) dx \quad \beta = \frac{2}{\alpha} \quad (2.18)$$

$$S_{HB} = \bar{S} + P_c \frac{d\bar{S}}{dP_{c1}} \quad (2.19)$$

This solution can be evaluated with high accuracy from discrete \bar{S} data using a simple differencing scheme (Appendix A). Using this scheme, solution S for each step is obtained directly from the values of \bar{S} . No smoothing or fitting of \bar{S} or averaging of S results are needed, but to prevent oscillation in processing of the experimental data, it is proposed to use physical constraints such as $S_j \leq S_{j-1}$.

The same solutions proposed for drainage can be similarly developed for imbibition, replacing:

$$B = 1 - \left(\frac{r_1}{r_3}\right)^2 \quad \text{by} \quad B = 1 - \left(\frac{r_3}{r_1}\right)^2 \quad (2.20)$$

The accurate approximate solution for imbibition is given by:

$$S(P_c) \approx S_\alpha(P_c) = \bar{S}(P_c) + \frac{P_c}{1+\alpha} \frac{d\bar{S}(P_c)}{dP_{c1}} \quad (2.21)$$

$$\alpha = \frac{1 - \sqrt{1-B}}{1 + 2\sqrt{1-B}} = \frac{r_3 - r_1}{r_3 + 2r_1} \quad B < 0 \quad (2.22)$$

Again, this solution can be evaluated with high accuracy from discrete \bar{S} data using a simple differencing scheme (Appendix A). Using this scheme, solution S for each step

is obtained directly from the values of \bar{S} . No smoothing or fitting of or averaging of S results are needed, but to prevent oscillation in processing of the experimental data, it is proposed to use physical constraints such as $S_j \geq S_{j-1}$ for $P_j \leq P_{j-1}$.

Forbes (Forbes 1994) has shown analytically for both drainage and imbibition that the S_{HB} approximation is always lower, and the S_D approximation is always higher than the exact solution:

$$S_{HB} \leq S \leq S_D \quad (2.23)$$

To sum up, the capillary pressure curves are established as follows:

1. Measurement of a data set (\bar{S}, ω) , \bar{S} being the average saturation of the specimen and ω the corresponding rotational speed.
2. Transformation of the measured data set into a data set (\bar{S}, P_c) , P_c being P_{c1} in equation (2.7) for drainage and P_{c3} in equation (2.11) for imbibition.
3. $S(P_c)$ is obtained by inverting the integral equation $\bar{S}(P_c)$ defined by equation (2.9) for drainage and equation (2.12) for imbibition.

Accounting for Gravity and Radial Effects

The calculation of the capillary pressure, which is similar for the Hassler-Brunner method, the van Domselaar method and the included Forbes method, only takes into account the centrifugal effect and not the radial effect or the effect of gravity. Including these effects results in the following capillary pressure equations (Forbes 1997).

For drainage, the capillary pressure is then given by:

$$P_{c1}(r, Z, \omega) = \frac{1}{2} \Delta \rho \omega^2 (r_3^2 - r_1^2) + \Delta \rho g Z + \frac{1}{2} \Delta \rho \omega^2 (n + 1) R^2 \quad (2.24)$$

where $n = 2(g/\omega^2)/R - 1$ if $g/\omega^2 > R$, or $n = (g/\omega^2)^2/R^2$ if $g/\omega^2 < R$. Similarly, for imbibition, the capillary pressure is then:

$$P_{c3}(r, Z, \omega) = \frac{1}{2} \Delta \rho \omega^2 (r_1^2 - r_3^2) + \Delta \rho g Z + \frac{1}{2} \Delta \rho \omega^2 (n + 1) R^2 \quad (2.25)$$

where $n = -2(g/\omega^2)/R - 1$.

By definition, the average saturation \bar{S} of the specimen can be found as:

$$\bar{S} = \frac{1}{L\pi R^2} \int_{specimen} S_{r,Z,\omega} dv = \frac{1}{L\pi R^2} \int_{specimen} S(P_c(r, Z, \omega)) dv \quad (2.26)$$

where L is the length of the specimen, R is the radius of the specimen, r is the rotational radius, Z is the vertical coordinate and dv is the elementary volume. $\bar{S}(P_c(r, Z))$ varies inside the core, and the above equation can be normalized and re-written into an expression denoted $\bar{S}_{B,N,M}(P_c)$ (Appendix B) depending on the parameters B (centrifugal effect), N (radial effect) and M (gravity effect). For the saturation solution in the Hassler-Brunner method given in equation (2.14), the pressure field is assumed linear (neither radial nor centrifugal), and the gravity is neglected: $B = 0$, $N = 0$ and $M = 0$. The

van Domselaar solution given in equation (2.15) and the included solutions by Forbes (Forbes 1994) given in equation (2.16) for drainage and equation (2.21) for imbibition neglect radial ($N = 0$) and gravity ($M = 0$) effects, but include centrifugal effects ($B \neq 0$).

To sum up, the capillary pressure curves accounting for gravity and radial effects are established as follows:

1. Measurement of a data set (\bar{S}, ω) , \bar{S} being the average saturation of the specimen and ω the corresponding rotational speed.
2. Transformation of the measured data set into a data set (\bar{S}, P_c) , P_c being P_{c1} in equation (2.24) for drainage and P_{c3} in equation (2.25) for imbibition.
3. $S(P_c)$ is obtained by inverting the integral equation $\bar{S}(P_c) = \bar{S}_{B,N,M}(P_c)$ defined in Appendix B.

Instead of performing a complicated inversion of the integral equation $\bar{S}_{B,N,M}(P_c)$, the equation is rewritten to provide an evaluation of the integral $\bar{S}_{B \neq 0, N=0, M=0}(P_c)$, for which inversion techniques are available (solutions to equation (2.9) for drainage and (2.12) for imbibition). A total correction accounting for both radial and gravity effects is then applied to the average saturation. Similarly, the total correction is applied to the calculation of P_c by equation (2.7) and (2.11) instead of using equation (2.24) and (2.25). This total correction consists of changing $(P_c, \bar{S}(P_c))$ by $(P_c/b, \bar{S}(P_c) + a_0(\bar{S}(a_0 P_c) - \bar{S}(P_c)))$ before processing the usual saturation solutions of equation (2.9) for drainage and equation (2.12) for imbibition (Forbes 1997). The correction parameters are included in Table 2.2 and Table 2.3.

	a_0	b_0
Drainage	$\frac{3/4N(1+(1-B)^{1/2})}{2(1+N)}$	$\frac{1+0.23N/(1+N)}{(1+N)}$
Imbibition	$\frac{-1/4N(1+(1-B)^{1/2})}{2}$	$\frac{1-a_0(4-(1-B)^{1/2})}{2+(1-B)^{1/2}}$

Table 2.2 Radial correction parameters (Forbes 1997).

	P_c	B	N	M	C	$1/b - 1/b_0$
Drainage	$\frac{1}{2}\Delta\rho\omega^2(r_3^2 - r_1^2)$	$\frac{(r_3^2 - r_1^2)}{r_3^2}$	$\frac{R^2}{(r_3^2 - r_1^2)}$	$\frac{g}{\omega^2 R}$	$\frac{N(4+2(1-B)^{1/2})}{(5+(1-B)^{1/2})}$	$M > 1 : (4M - 1.75)C$ $0 < M < 1 : 2.25M^{1.7}$
Imbibition	$\frac{1}{2}\Delta\rho\omega^2(r_1^2 - r_3^2)$	$\frac{(r_1^2 - r_3^2)}{r_1^2}$	$\frac{R^2}{(r_1^2 - r_3^2)}$	$\frac{-g}{\omega^2 R}$	$\frac{N(4+2(1-B)^{1/2})}{(5+(1-B)^{1/2})}$	$M < 0 : 4MC$

Table 2.3 Correction parameters (Forbes 1997).

B represents the centrifugal effects related to the fact that the capillary pressure varies with r^2 and not linearly with r . N represents the magnitude of radial effects related to

the curvature of the capillary pressure field around the rotational axis. M is "a priori" an appropriate parameter to measure the effect of gravity.

Centrifuge Bond Number

De-saturation effects, i.e. mobilization of trapped nonwetting phase (residual saturation), can cause changes in capillary pressure curves established at high flow rates. The capillary pressure curves will change as the residual saturation is changed. De-saturation effects (usually) do not occur under normal field conditions. To avoid these effects, the critical Bond number (ratio between gravitational and capillary forces) should not be exceeded (Verbruggen et al. 2000). This Bond number requirement implies an upper limit for the centrifugal acceleration due to that the gravitational (here centrifugal) forces are stronger than the capillary forces when spinning the centrifuge at high speeds.

The dimensionless centrifuge Bond number $N_{B, cen}$ describes the ratio of centrifugal to capillary forces (Skauge & Poulsen 2000):

$$N_{B, cen} = \frac{K\omega^2 r \Delta\rho}{\sigma_i} \quad (2.27)$$

where K [m^2] is the absolute permeability, ω [sec^{-1}] is the rotational speed, r [m] is the radius from the centre of the specimen to the rotational axis, $\Delta\rho$ [kg/m^3] is the fluid density difference and σ_i [mN/m] is the interfacial tension between the two fluids. This expression transforms into the conventional gravity-to-capillary Bond number, N_B , by replacing the centrifugal acceleration $\omega^2 r$ with the gravitational acceleration g .

At low centrifugal speed, the flow regime is capillary dominated, and the trapped phase is not mobilized. Above the critical centrifuge Bond number (the critical value of rotational speed), at which centrifugal forces dominates over capillary forces, the nonwetting phase is mobilized.

The dimensionless centrifuge Bond number $N_{B, cen}$ are calculated to be in the range of $9.7 \cdot 10^{-12}$ to $1.3 \cdot 10^{-9}$ for a mean absolute, permeability of $K = 2.8 \cdot 10^{-15} \text{ m}^2$ (mean value of 2.6-2.9 mD), a difference in density of oil and water of $\Delta\rho = 287 \text{ kg}/\text{m}^3$ and an interfacial tension between oil and water of $\sigma_i = 60 \text{ mN}/\text{m}$.

The calculated range of the centrifuge Bond number is below the critical centrifuge Bond number of 10^{-5} for Maui BD oil sands. Since the matrix permeability around 2-3 mD for Hillerslev outcrop chalk is significantly lower than for the reference low-permeable sandstone, no conclusions can be made. However, the author has located no critical centrifuge Bond number for avoiding de-saturation effects in chalk.

Chapter 3

Description of the Laboratory Tests

Wettability and capillary pressure measurements were performed on three Hillerslev outcrop chalk specimens 1, 2 and 3 at Rogaland Research, Stavanger, Norway. This was done by utilizing Amott cups and an automated Beckman centrifuge. The laboratory journal is included, see Appendix C.

All saturation calculations are based on a volume balance except for the initial fully saturation of specimens 1 and 2 with water and specimen 3 with Isopar-L, which is based on weights. In addition to the volume balance, weighing of the specimens has been performed after each step as check.

3.1 Hillerslev Chalk Specimens and Fluids

The three specimens were taken from a small block of Hillerslev outcrop chalk material from the earlier research project "Fractures and Rock Mechanics", phase 2 (Jakobsen 2001). The specimens were drilled using a water-cooled $\varnothing 42$ drill. The specimens were dried in an oven at 105°C.

The specimens were turned in a turning lathe to a diameter of approximately 3.8 cm and then both ends of the specimens were cut by an electric saw to a length of approximately 5.0 cm. The specimens were described, measured and sketched, see Appendix D.

Specimen 1

The aim was to obtain a less water-wet specimen containing Isopar-L and with an initial water saturation in order to resemble the conditions of the Tor formation of the Valhall field.

Hillerslev chalk is regarded as a close analogue to chalk from the Tor formation of the Valhall field. The chalk from the Tor formation is reported to be neutral- to slightly oil-wet with an initial water saturation of about 5%. The Amott-Harvey wettability index is in the range of 0 to -0.37 (Andersen, 1995). The chalk from the Tor formation is also reported to be neutral- to slightly water-wet (Eltvik et al. 1990).

Specimen 2

The aim was to obtain a water-wet specimen containing Isopar-L and with an initial water saturation in order to resemble laboratory conditions for prior tests on Hillerslev chalk.

Specimen 3

The aim was to obtain a water-wet specimen saturated with Isopar-L in order to resemble laboratory conditions for prior tests on Hillerslev chalk, and compare test results for specimens with and without initial water saturation.

Fluids

Due to the composition of the laboratory oil Isopar-L, Hillerslev outcrop chalk saturated with Isopar-L stay water-wet. The density of Isopar-L is 0.763 g/cm^3 and the viscosity is 1.41 cP , both at 22°C .

The water used was synthetic formation water, which was mixed using a recipe for the Valhall field formation water. The recipe for the water (g/2 l distilled water) is shown in Table 3.1. Small pieces of chalk were put into this mixture to prevent dissolution of the specimens. In this report, the synthetic formation water is referred to as water. The density of the water is 1.05 g/cm^3 and the viscosity is 1.0 cP , both at room temperature. The interfacial tension between Isopar-L and the water is 60 mN/m (GEUS).

NaCl	121.76 g/2 l
KCl	0.48 g/2 l
CaCl ₂	29.5 g/2 l
MgCl ₂ × 6H ₂ O	9.1 g/2 l

Table 3.1 Recipe for the synthetic Valhall field formation water.

3.2 Preparation of the Specimens

The specimens were dried in an oven at 105°C . Then a shrink-fix sleeve was put around each specimen, and this was heated with a heating pistol and cut at both ends to fit the periphery of the specimen. Shrink-fix sleeves were used to ensure that fluid only enters and leaves through the end-faces of the specimens. Further, shrink-fix sleeves also makes the specimens more stabile in order to be able to withstand the rough treatment in the centrifuge.

Pressure heads and porous plates were placed in both ends of the specimen, and a rubber membrane was placed around the specimen and the pressure heads. There are channels in the pressure heads for an even distribution of injected fluids and to ease collection of displaced fluids. The length of the specimen was adjusted with rubber disks to fit the rubber membrane. The membrane was fixed at both ends with cobber wire. The specimen was then placed in an Exxon Triaxial core holder. One of the pressure

heads was fitted into the core holder and was thus a fixed part of the core holder while the other was part of a piston, see Figure 3.1. Isopar-H was sent into the core holder via a pump to obtain a pressure of 20 bar on the membrane around the specimen in order to prevent flow along the side of the specimen.

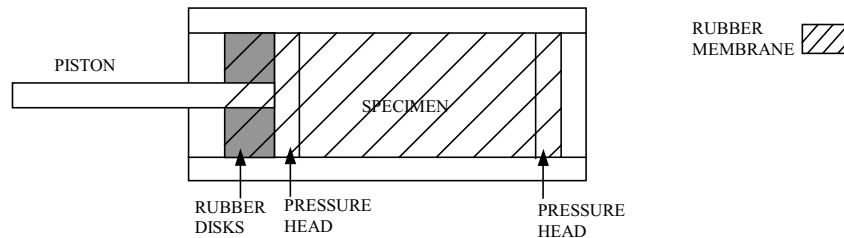


Figure 3.1 Specimen placed in the Exxon Triaxial core holder.

Specimens 1 and 2 were initially fully saturated with water, and specimen 3 was initially fully saturated with Isopar-L. The set-up for the initial fully saturation of the specimens is seen in Figure 3.2.

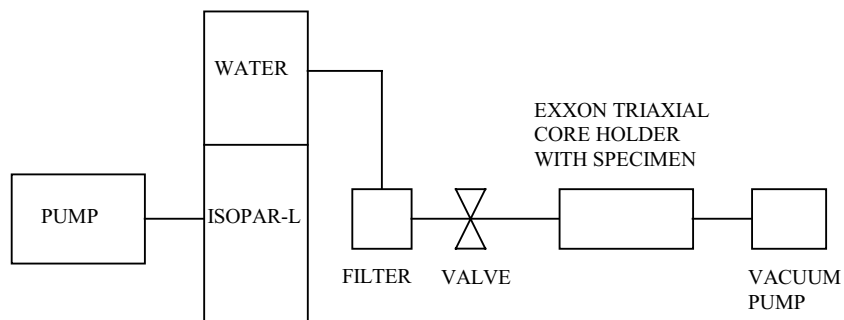


Figure 3.2 Set-up for initial fully saturation of the specimens.

A 10 bar reference pressure was applied for the initial fully saturation of the specimens (pump: 20 bar and vacuum pump: 10 bar). Then the specimens were flushed (0.5 ml/min.) with a backpressure of 10 bar applied in order to remove air from the specimens. A filter was put into the set-up ($0.45 \mu\text{m}$) to prevent pieces of chalk in the water above the filter size to enter the specimens. The mean absolute water permeability of specimens 1 and 2 was measured during flushing to 2.6-2.9 mD, see Appendix E.

After saturation, the specimens were taken out of the core holders and weighed. The wettability of specimen 1 was to be altered to a less water-wet state. Specimen 3 was placed in a container with Isopar-L and left until the aging period of specimen 1 was over.

To obtain low initial water saturations in specimens 1 and 2, the high viscous laboratory oil Marcol was used to displace the water, see Figure 3.3. First the specimens were flushed with the low viscous Isopar-L in order to establish a channel through the specimen

(flushing until breakthrough). This was done to avoid a high differential pressure over the specimen or a low injection rate when flushing with Marcol. The specimens were then flushed with Marcol to displace the water in place. Then the specimens were flushed with Isopar-L (0.1-0.2 ml/min.) to displace the Marcol. Specimen 2 was then placed in a container with Isopar-L and left until the aging period of specimen 1 was over.

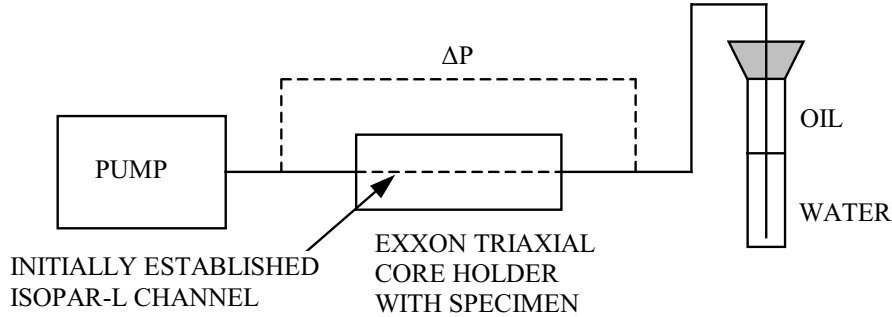


Figure 3.3 Set-up for establishment of initial water saturation (specimens 1 and 2).

The initial parameters for the three chalk specimens after saturation are shown in Table 3.2.

The mean diameter D [cm], height H [cm] and dry weight M_{dry} [g] are measured. The bulk volume BV [cm³] is calculated as $\pi(D/2)^2H$. The dry density ρ_{dry} [g/cm³] is calculated as M_{dry}/BV . The void ratio e [-] is calculated as $\rho_s/\rho_{dry} - 1$, where the chalk grain density is $\rho_s = 2.70$ g/cm³. The porosity ϕ [%] is calculated as $e/(e + 1) \cdot 100$. The pore volume PV [cm³] is calculated as $\phi \cdot BV$.

The fully saturation of specimens 1 and 2 with water and specimen 3 with Isopar-L is based on weights, i.e. $(M_{sat} - M_{dry})/\rho_{fluid}/PV \cdot 100$ with a water density of $\rho_w = 1.05$ g/cm³ and an oil density of $\rho_o = 0.763$ g/cm³. The air saturation is found as $100 - S$.

The initial water saturations for specimens 1 and 2 are obtained from the amount of displaced water, i.e. $(M_{sat} - M_{dry} - M_{disp})/\rho_w/PV \cdot 100$. The air saturation is assumed constant $S_a = S_{ai}$, and the initial oil saturation is found as $100 - S_{wi} - S_{ai}$.

The initial water saturation of specimen 1 is much lower than for specimen 2 although the aim was to obtain the irreducible water saturation S_{wir} in both specimens. The difference may be due to inhomogeneities in the chalk specimens or the procedure followed to obtain S_{wir} . In the following, the specimens are being referred to as having an initial water saturation S_{wi} , and not irreducible water saturations.

Wettability Alteration

The crude oil used for aging of specimen 1 was oil from the Snorre field in the North Sea (Norsk Hydro). The crude oil must have an AN in the order of 0.5-1.0 mg KOH/g oil if the chalk wettability is to be altered towards oil-wet (personal communication with Professor Tor Austad, Stavanger College, Norway). However, it was not possible to obtain information about the acid number (AN) for the Snorre oil. To ensure the ability of the oil to alter the wettability towards less water-wet, it was decided to add 1 weight%

Specimen	1	2	3
Mean diameter, D [cm]	3.81	3.80	3.81
Mean height, H [cm]	5.00	5.00	5.00
Dry weight, M_{dry} [g]	82.03	81.74	81.70
Bulk volume, BV [cm ³]	57.00	56.71	57.00
Dry density, ρ_{dry} [g/cm ³]	1.44	1.44	1.43
Void ratio, e [-]	0.88	0.88	0.89
Porosity, ϕ [%]	46.8	46.8	47.1
Pore volume, PV [cm ³]	26.68	26.54	26.85
Fully saturation with water or oil			
Weight after water or oil saturation, M_{sat} [g]	108.67	109.30	101.72
Water or oil saturation, S [%]	95.1	98.9	97.7
Air saturation, S_a [%]	4.9	1.1	2.3
Initial water saturation in specimens 1 and 2			
Displaced water, M_{disp} [g]	23.05	19.46	-
Initial water saturation, S_{wi} [%]	12.8	29.1	-
Initial oil saturation, S_{oi} [%]	82.3	69.8	97.7
Initial air saturation, S_{ai} [%]	4.9	1.1	2.3
Absolute water permeability, K [mD]	2.9	2.6	-

Table 3.2 *Initial parameters for the three Hillerslev chalk specimens.*

Dodekane acid ($C_{11}H_{23}COOH$) to the oil (personal communication with Professor Tor Austad, Stavanger College, Norway).

In order to obtain a homogenous wettability state throughout the chalk specimen, the specimen was flushed with 100 ml Snorre oil added 1 weight% Dodekane acid in each direction at a rate of 0.1-0.2 ml/min. The content of wax in crude oil can have some kind of blocking effect due to precipitation of wax in the porous media. Generally, if the temperature is above 40°C there are no problems with the wax. The flushing, though, was performed at room temperature. After flushing, the specimen was aged for 5 weeks at 90°C and 8 bar in a piston cell. The oil mixture surrounded the ends of the specimens, but it was not possible to surround the periphery of the specimens with this mixture due to the shrink-fix sleeves.

After 5 weeks of aging, specimen 1 (referred to as 1A in the following) was removed from the piston cell. The specimen broke in one end as it was removed. The specimen was now brittle, and the colour was changed to dark brown. Specimen 1A was placed in the Exxon Triaxial core holder and 20 bar pressure was applied to prevent flow along the side. The core holder was placed in the set-up shown in Figure 3.2, and the crude oil was displaced by Isopar-L. This was done at 40°C to prevent wax effect. The specimen was flushed with Isopar-L at a rate of 0.1-0.2 ml/min. After displacement of the crude oil, the periphery of specimen 1A was slightly uneven. The broken end was cut to an even surface, and the outermost layer (approximately 2 mm) of the other end was removed. A new height was measured. Under the assumption that the porosity, dry density and fluid

saturations were unchanged, a new mean diameter and thus a new bulk volume and pore volume were calculated, see Table 3.3.

Specimen	1A
Mean diameter [cm]	3.79
Mean height [cm]	3.62
Bulk volume [cm ³]	40.84
Pore volume [cm ³]	19.12

Table 3.3 *New parameters for specimen 1A.*

The wettability alteration seemed to have affected the structure of specimen 1A, and the calculation revealed a slightly lower mean diameter. However, it was chosen to use specimen 1A in the wettability and capillary pressure measurements to test a chalk specimen altered by this procedure. Further, the author was given the opportunity at Rogaland Research to carry out measurements on three chalk specimens, and no additional Hillerslev outcrop chalk specimen was available at the time.

3.3 Test Procedure

Measurement of wettability and capillary pressure was performed on the three Hillerslev outcrop chalk specimens. This was done by utilizing Amott cups and an automated Beckman centrifuge. The modified USBM method was used to obtain both the Amott-Harvey and the USBM wettability indices, and based on the measurements, water-oil capillary pressure curves were established for the three specimens. The modified USBM test procedure consists of the 5 steps listed in Table 3.4.

Step 1	Establish S_{wir} (specimens 1 and 2)
Step 2	Submerge the specimens in water and record the production of oil
Step 3	Centrifuge the specimens in water and record the production of oil
Step 4	Submerge the specimens in oil and record the production of water
Step 4	Centrifuge the specimens in oil and record the production of water

Table 3.4 *The test procedure for the wettability and capillary pressure measurements.*

Instead of establishing an irreducible water saturation S_{wir} by use of the centrifuge (step 1), an initial water saturation S_{wi} was established in specimens 1 and 2 (Section 3.2), and specimen 3 had no initial water.

After establishment of an initial water saturation S_{wi} (step 1), the specimens were immersed in water in Amott cups, and the volume of water imbibing spontaneously was measured as the volume of oil displaced (step 2). Then the specimens were centrifuged to force water into the specimens, and the average saturation of the specimens was determined from the volume of expelled oil at each incremental capillary pressure. After

centrifuging, the specimens were left at (or close to) the residual oil saturation S_{orw} (step 3). Then the specimens were immersed in oil, and the volume of oil imbibing spontaneously was measured as the volume of water displaced (step 4). Finally, the specimens were centrifuged to force oil into the specimens, and the average saturation of the specimens was determined from the volume of expelled water at each incremental capillary pressure (step 5). After centrifuging in oil, the specimens were supposed to be left at the irreducible water saturation S_{wir} , but due to centrifuge speed limitations, the water saturation after centrifuging S_w is assumed higher than S_{wir} . However, S_w was lower than S_{wi} for specimens 1 and 2.

Amott Cups

The specimens were placed in Amott cups, see Figure 2.3. A spiral made with cobber wire was placed under the specimens so that the specimens were not standing directly on the bottom, i.e. there was space under the specimens for fluid to be displaced. The amount of displaced volume was read on the calibration lines at the top of the Amott cup. The use of shrink fix sleeves delays both the imbibition and the drainage due to that these processes only take place at the end-faces of the specimens. The fluid was displaced as drops that were formed at the top and bottom ends of the specimens, and released or pushed free by use of a cobber wire.

Beckman Centrifuge

The capillary pressure measurements were performed at Rogaland Research in a Beckman L8-55M/P Ultra centrifuge using a rotor with standard or inverted buckets (Pub 1983). Three 1.5" diameter cylindrical specimens can be centrifuged simultaneously in the Beckman centrifuge. The centrifuge is automated so that there is automatic reading of produced volumes, evaluation of equilibrium, and change of speed.

This centrifuge is equipped with a strobe light assembly in the rotor chamber door. The strobe flashes once during each revolution of the rotor, so measurement of extracted volume can be made without stopping the centrifuge. The strobe can be adjusted to shine through a slit in any one of the rotor buckets. The extracted fluid is collected in a tube. A camera reads the produced fluid volume and a stroboscope light ensures that the camera obtains stable recordings in the rotation cup.

In the centrifuge, multi-step tests were performed, i.e. the angular velocity was increased in steps. The produced volumes at each step were read every 1-2 seconds initially, but as the production slowed down, the readings were every 5 minutes. At each step, the centrifuge was spun until hydrostatic equilibrium was reached. In the tests, equilibrium was defined as the point at each step for each specimen where the fluid production was $\leq 0.03 \text{ cm}^3$ over a 5 minutes period. However, the data processing revealed that the hydrostatic equilibrium may have been defined at too high a fluid production level, as the production curves were not constant in every step. A small production of 0.03 cm^3 or less went on for a long period of time in some of the specimens at some of the steps. These steps should have been allowed to carry on for a longer period of time. The centrifuge tests were performed at 40°C to ensure that there was no problem with wax in specimen 1A.

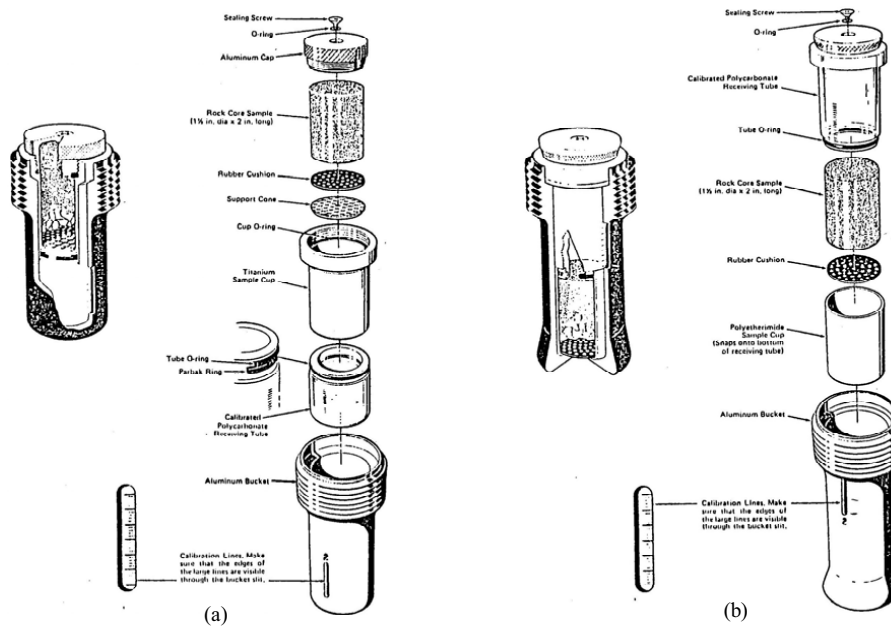


Figure 3.4 Mounting of specimens in (a) standard buckets and (b) inverted buckets (Pub 1983).

The specimens were mounted in the centrifuge cups, and an amount of the displacing fluid was poured into the cups. A separating disk was put into each cup to make the water and oil separation visible. As indicated in Figure 3.4, the centrifuge cups are placed inside the centrifuge buckets. The standard buckets are used for forced displacement of water by oil and the inverted buckets are used for forced displacement of oil by water.

A set-up for the centrifuge tests is shown in Figure 3.5. In the standard buckets, surrounding oil enters the specimen at the inlet face and displaces water at the outlet face. In the inverted buckets, surrounding water enters the specimen at the inlet face and displaces oil at the outlet face.

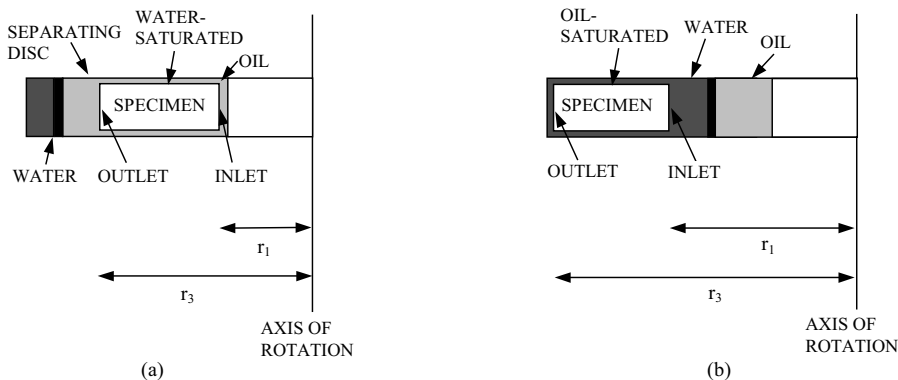


Figure 3.5 (a) displacement of water by oil in a standard bucket (oil drive) and (b) displacement of oil by water in an inverted bucket (water drive).

Chapter 4

Laboratory Test Results

The measured total spontaneous displaced volumes in the Amott cups and the measured total forced displaced volumes for the oil drive and the water drive in the centrifuge are included in Table 4.1. Only the total amounts of spontaneous displaced volumes are included. The production curves for the centrifuge tests, i.e. plots of the measured corresponding values of centrifuge speed and produced volumes are shown in Appendix F.

4.1 Wettability Determination

Both the Amott-Harvey and the USBM wettability indices can be determined from the modified USBM method. The capillary pressure vs. average saturation is plotted for specimens 1A, 2 and 3 to obtain the USBM wettability index, see Figure 4.1, 4.2 and 4.3, respectively. The capillary pressure is calculated using equation (2.7) for drainage and equation (2.11) for imbibition. The average water saturation is calculated as $\bar{S} = V_{water}/PV$ based on the measured production data, where V_{water} is the total volume of water present in the specimens and PV is the pore volume.

The small amount of spontaneous oil imbibition $\Delta S_{Oimb} = 0.12 \text{ cm}^3$ for specimen 1A with a pore volume of 19.12 cm^3 and an initial water saturation of $S_{wi} = 12.8\%$ is indicated in Figure 4.1. The area A_1 under the oil-drive curve, and the area A_2 above the water-drive curve are indicated as well, both bounded by a capillary pressure of 70 kPa defined for the calculation of the USBM wettability index (Section 2.1). The USBM wettability index for specimen 1A is included in Table 4.1.

The spontaneous water imbibition $\Delta S_{Wimb} = 10.8 \text{ cm}^3$ for specimen 2 with a pore volume of 26.55 cm^3 and an initial water saturation of $S_{wi} = 29.1\%$ is indicated in Figure 4.2.

The spontaneous water imbibition $\Delta S_{Wimb} = 19.3 \text{ cm}^3$ for specimen 3 with a pore volume of 26.84 cm^3 and no initial water saturation is indicated in Figure 4.3.

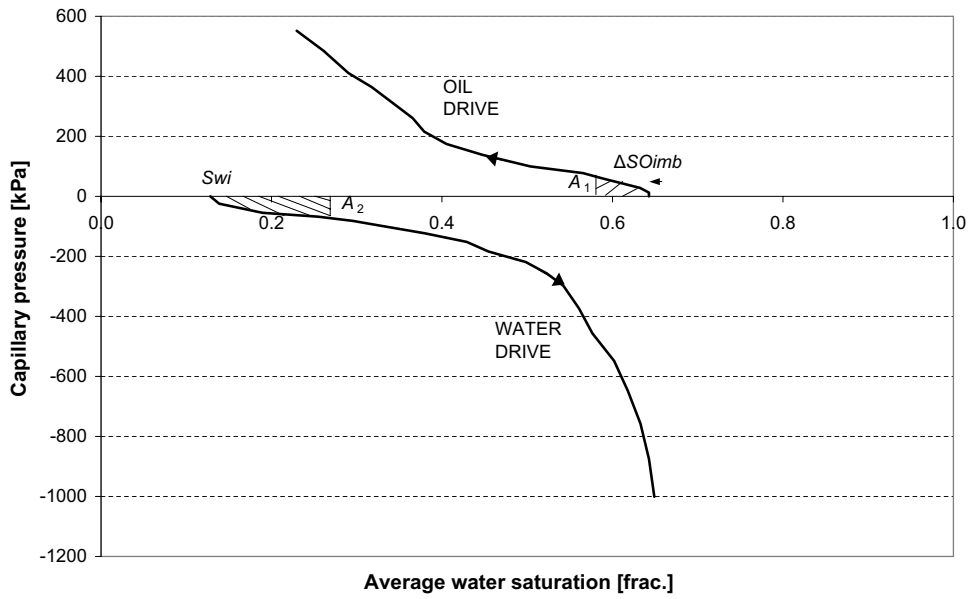


Figure 4.1 Wettability measurement by the modified USBM method for specimen 1A.

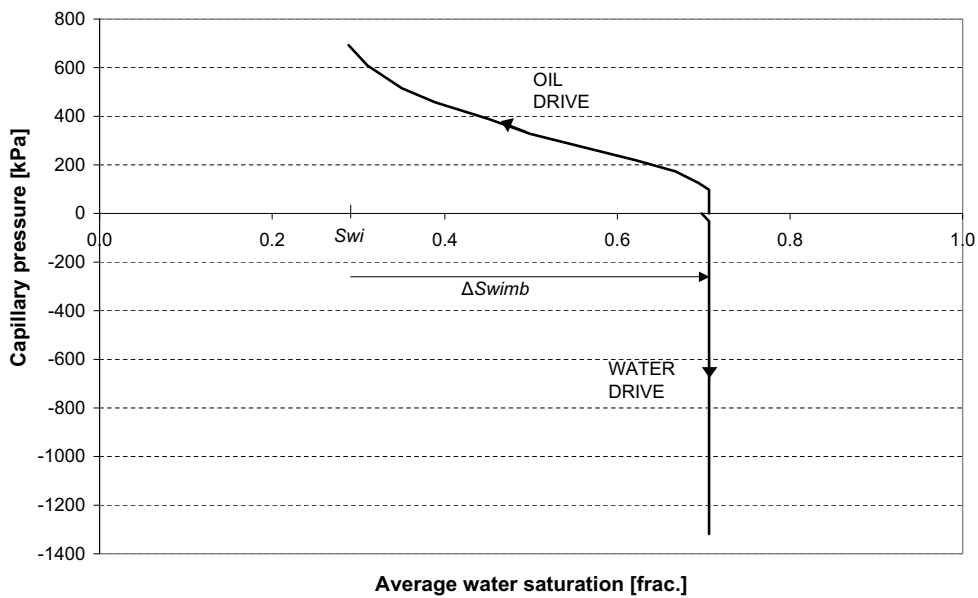


Figure 4.2 Wettability measurement by the modified USBM method for specimen 2.

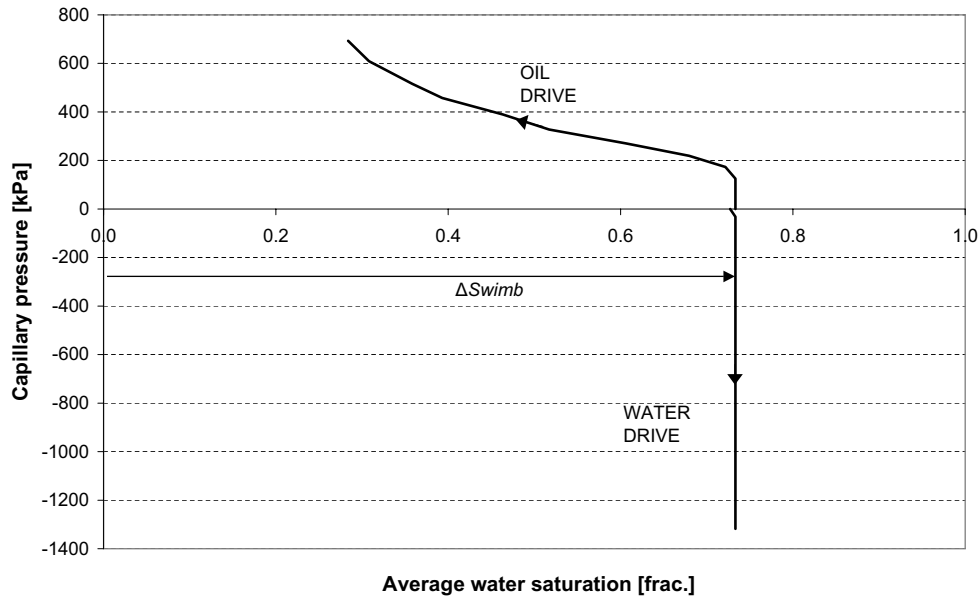


Figure 4.3 Wettability measurement by the modified USBM method for specimen 3.

It was not possible to calculate the USBM wettability index for specimens 2 and 3 since the minimum capillary pressure required to force oil into the specimen (oil drive) was higher than the upper boundary of 70 kPa defined for the USBM wettability index calculation, i.e. no area A_1 under the oil-drive curve can be found below the capillary pressure boundary of 70 kPa. The area A_2 above the water drive curve is zero since no water could be forced into specimens 2 and 3 after spontaneous water imbibition, see Table 4.1.

The small initial increase in S_w seen on the water drive curves for specimens 2 and 3 is calculated to be due to water displacing air in the matrix during the initial centrifuging, see Table 4.2.

The oil drive for all three specimens implies that the centrifuge test was ended at too low a capillary pressure. In other words, these capillary pressure curves were not fully completed due to centrifuge speed limitations even though the Beckman centrifuge was run to its maximum capacity of 8000 RPM. This means that the irreducible water saturation S_{wir} was not obtained in any of the specimens at the end of the test.

In the Amott test, the specimens are supposed to start at S_{wir} and end at S_{wir} . However, it is stated that the ratio of spontaneous to forced imbibition is used to reduce the influence of factors such as relative permeability, viscosity and the initial saturation of a specimen (Anderson 1986a). So although it is evaluated that S_{wir} was not obtained initially in any of the three specimens, the specimens are still used for the wettability measurements. Due to centrifuge speed limitations, the irreducible water saturation was also not obtained at the end of the measurements. However, the water drive for specimen 1A implies that the specimen is close to the residual oil saturation S_{orw} before the oil drive, and S_{orw} is obtained in specimens 2 and 3, since no more water could be forced

Specimen	1A	2	3
Establishment of S_{wi}			
S_{wi} (average)	12.8	29.1	-
Amott/USBM wettability test			
Amott cup step 2, oil production [cm ³]	0.0	10.8	19.3
S_w (average)	12.8	69.8	71.9
Centrifuge step 3, oil production [cm ³]	9.2	0.0	0.0
S_w (average)	63.9	70.6	73.3
Amott cup step 4, water production [cm ³]	0.12	0.0	0.0
S_w (average)	63.2	70.6	73.3
Centrifuge step 5, water production [cm ³]	7.80	11.09	12.06
S_w (average)	22.4	28.8	28.4
Amott/USBM wettability index			
$WWI = 2/(2+3)$	0	1	1
$OWI = 4/(4+5)$	0.02	0	0
Amott-Harvey $WI = WWI - OWI$	-0.02	1	1
USBM WI	-0.77	-	-

Table 4.1 Capillary pressure measurements and wettability index determination.

into the specimens after spontaneous water imbibition. The fact that S_{wir} was neither obtained initially nor at the end of the measurements have no influence on the Amott-Harvey wettability index for specimens 1A, 2 and 3 nor on the USBM wettability index for specimens 2 and 3. A lower S_{wi} in specimen 1A may have resulted in a larger area A_2 and thus a higher USBM wettability index, i.e. more oil-wet, since no water imbibed spontaneously.

It is obvious from the Amott cup displacement results that a wettability alteration of specimen 1A is obtained. For specimen 1A, the Amott-Harvey wettability index is calculated to -0.02, i.e. slightly oil-wet (near neutral). The produced amount of water in the Amott cup $\Delta S_{Oimb} = 0.12 \text{ cm}^3$ equals less than 1% of the pore volume of specimen 1A, and this could be a result of exchange of fluids on the surface implying no spontaneous oil imbibition, and thus a neutral-wet state. However, it is evaluated that the small amount of oil imbibed. The fact that a part of one end of the specimen broke off eliminates the risk of outermost effects at that end, and 2 mm was removed at the other end.

The USBM wettability index for specimen 1A is calculated to -0.77. The USBM wettability index supports specimen 1A being oil-wet. Specimen 1A is not considered fractional-wet (at least not at the ends where the displacement takes place) as water did not imbibe spontaneously whereas a small amount of oil imbibed spontaneously. Although the USBM wettability index indicates a moderately oil-wet state, the fact that only little spontaneous oil imbibition occurred implies that the specimen is less than moderately oil-wet.

Based on these considerations, it is evaluated that the wetting state of specimen 1A is neutral to slightly oil-wet. It is thus evaluated that the USBM wettability index over-

Specimen	1A			2			3		
	\bar{S}_w [%]	\bar{S}_o [%]	\bar{S}_a [%]	\bar{S}_w [%]	\bar{S}_o [%]	\bar{S}_a [%]	\bar{S}_w [%]	\bar{S}_o [%]	\bar{S}_a [%]
Initial	12.8	82.3	4.9	29.1	69.8	1.1	0.0	97.7	2.3
Amott (water)	12.8	82.3	4.9	69.8	29.1	1.1	71.9	25.9	2.3
Centrifuge (water)	63.9	34.1	2.0	70.6	29.1	0.3	73.3	25.9	0.8
Amott (oil)	63.2	34.8	2.0	70.6	29.1	0.3	73.3	25.9	0.8
Centrifuge (water)	22.4	75.6	2.0	28.8	70.9	0.3	28.4	70.8	0.8

Table 4.2 Average fluid saturation data throughout the test for specimens 1A, 2 and 3.

estimates the wettability towards oil-wet for the wettability altered specimen, i.e. there is a problem using the USBM method for the wettability altered Hillerslev outcrop chalk specimen.

Hillerslev outcrop chalk and hereby specimens 2 and 3 were assumed water-wet prior to testing, but the wettability measurement can be used to determine the degree of water-wetness. For specimens 2 and 3, water imbibed rapidly, and approximately 88% of the spontaneous imbibition was completed within an hour. After spontaneous imbibition, the specimens were at the residual oil saturation S_{orw} as no water could be forced into the specimens by use of the centrifuge. This indicates, that the specimens are strongly water-wet. This is supported by the fact that the Amott-Harvey wettability index was calculated to 1.

The overestimation of the USBM wettability index for specimen 1A, and the fact that the USBM wettability index could not be obtained for the water-wet specimens 2 and 3 does not imply problems using the centrifuge for capillary pressure measurements. However, it does imply that the USBM method for obtaining the USBM wettability index cannot be used for Hillerslev outcrop chalk. To the authors knowledge, the USBM method was developed for sandstone and not chalk.

The average saturations obtained at each of the 5 steps in the combined Amott-Harvey and USBM test for all three specimens are included in Table 4.2. All saturation calculations are based on a volume balance except for the initial saturations, which are based on weights. In addition to the volume balance, weighing of the specimens has been performed after each step as check. The change in average air saturation is calculated to be due to water replacing air during the initial centrifuging of the specimens.

A comparison of the saturations for specimens 2 and 3 shows that for (these) strongly water-wet specimens, the water imbibition potential is equal, i.e. the average water saturation after spontaneous (and forced) water imbibition is approximately the same for the two specimens in spite of the difference in initial water saturation. Further, after test the specimens reach approximately the same final average water saturation.

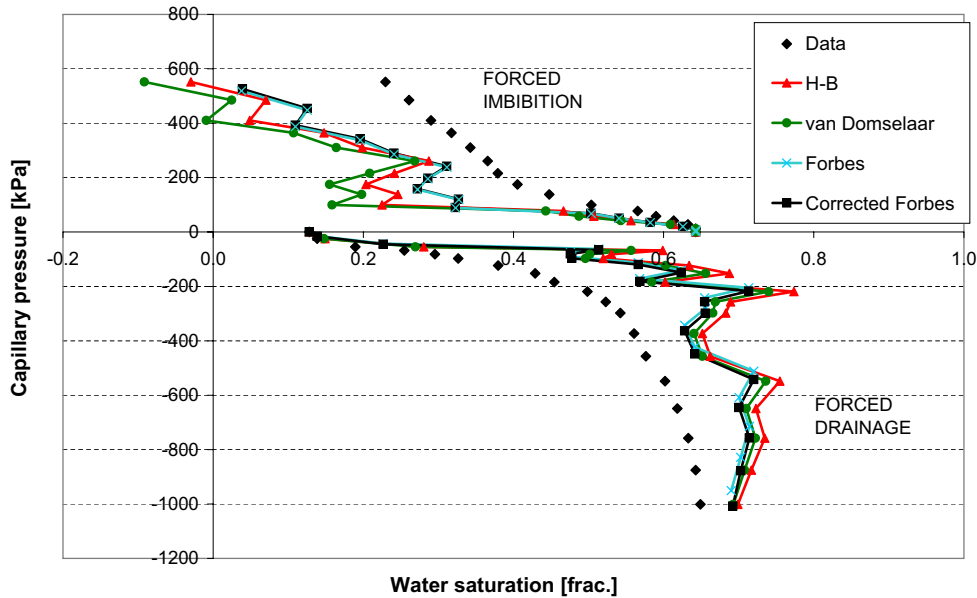


Figure 4.4 *Water-oil capillary pressure curves for specimen 1A for all data. The end-face saturations are calculated based on the Hassler-Brunner, the van Domselaar and the Forbes solutions. The corrected capillary pressure curves obtained by the Forbes method are included. The corresponding capillary pressure and average saturation are included (referred to as data).*

4.2 Capillary Pressure Curves

Since the wettability of the specimens has now been determined, the capillary pressure curves can be established from the centrifuge data obtained during the modified USBM test although to capillary pressures above 70 kPa. During the modified USBM centrifuge method, the centrifugal capillary pressures are calculated for all three specimens using equation (2.7) for drainage and equation (2.11) for imbibition.

The capillary pressure curves are based on the saturation at the end-face of the specimens, which is calculated from the average saturation. The end-face saturation is calculated on basis of the Hassler and Brunner solution (Hassler & Brunner 1945) equation (2.14), the van Domselaar solution (Forbes 1994) equation (2.15), and also the Forbes solution (Forbes 1994) equation (2.16) for drainage and equation (2.21) for imbibition. These end-face saturation solutions are uncorrected, i.e. there are not accounted for radial and gravity effects, and for the Hassler and Brunner solution there is not accounted for centrifugal effect either. The corresponding values of capillary pressure and end-face saturation obtained by the three different methods are plotted for the three specimens in Figure 4.4, 4.5 and 4.6. Only corresponding values of centrifugal capillary pressure and end-face saturation, i.e. only forced imbibition and forced drainage are included. The corresponding values of capillary pressure and average saturation are plotted as well (referred to as data). Further, the capillary pressure curves obtained by the Forbes method are corrected for radial and gravity effects, and the corrected capillary pressure curves are also included.

The capillary pressure curves for specimen 1A are plotted under the assumption that

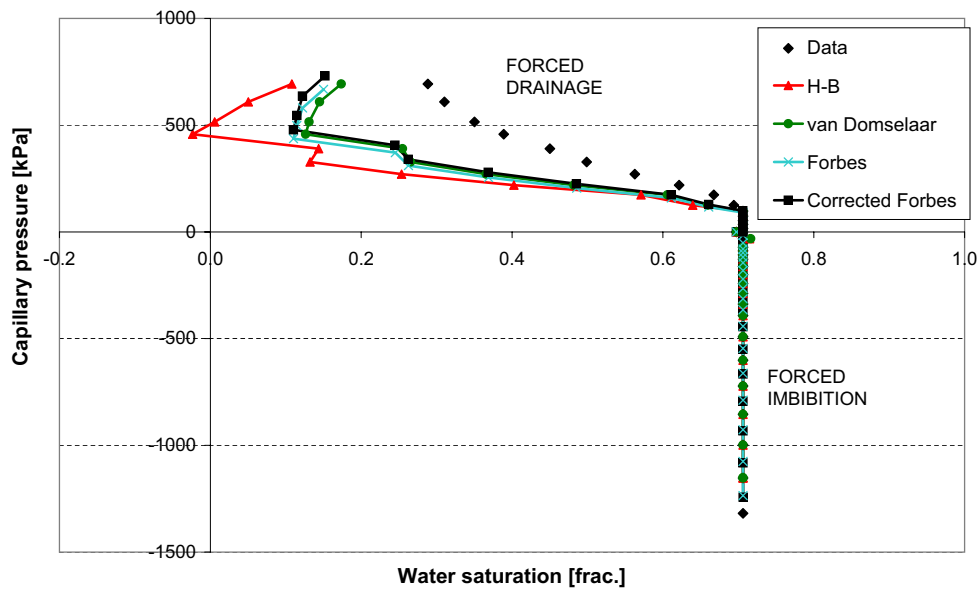


Figure 4.5 Water-oil capillary pressure curves for specimen 2 for all data. The end-face saturations are calculated based on the Hassler-Brunner, the van Domselaar and the Forbes solutions. The corrected capillary pressure curves obtained by the Forbes method are included. The corresponding capillary pressure and average saturation are included (referred to as data).

the specimen is neutral to slightly oil-wet. However, the capillary pressure is plotted as a function of the water saturation, i.e. the nonwetting phase saturation. The calculated capillary pressure curves consist of oscillating points. The main reason for this is that the production for some of the centrifuge steps was not constant at the defined hydrostatic equilibrium. The hydrostatic equilibrium may thus have been defined at too high a fluid production level, i.e. these steps were ended too soon.

For specimen 1A, $r_1/r_3 = 0.6$ for imbibition implies that the capillary pressure curves for the Hassler-Brunner method and the van Domselaar method ($r_1/r_3 \geq 0.7$) may not be accurate enough. For drainage, $r_1/r_3 = 0.8$ and the methods may be accurate enough.

The capillary pressure curves for specimens 2 and 3 are established knowing the specimens are strongly water-wet. The drainage part of the capillary pressure curves for both specimens 2 and 3 consists of oscillating points. The main reason for this is that the production for some of the centrifuge steps was not constant at the defined hydrostatic equilibrium. For both specimens, the forced imbibition curves are straight lines as no water could be forced into the specimens after spontaneous imbibition of water.

For specimens 2 and 3, $r_1/r_3 = 0.7$ for imbibition implies that the capillary pressure curves obtained by the Hassler-Brunner method and the van Domselaar methods may be accurate enough, but $r_1/r_3 = 0.5$ for drainage implies that the methods may not be accurate enough.

The capillary pressure curves obtained by the three different methods for the three specimens all consist of oscillating points, and have similar trends, although the solution proposed by Forbes (Forbes 1994) was reported to allow for conversion of sparse and noisy experimental data without smoothing, fitting, averaging, or forcing data to a given form.

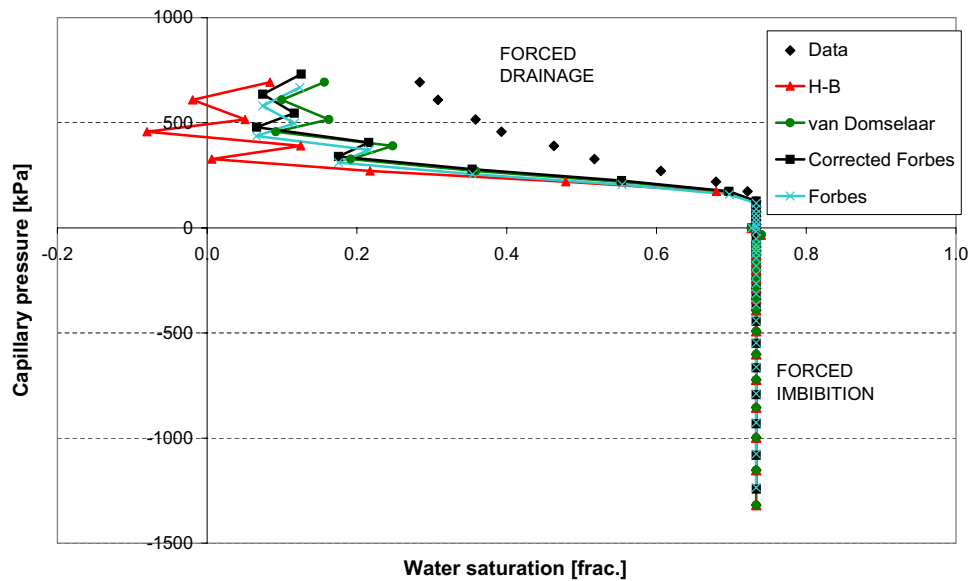


Figure 4.6 Water-oil capillary pressure curves for specimen 3 for all data. The end-face saturations are calculated based on the Hassler-Brunner, the van Domselaar and the Forbes solutions. The corrected capillary pressure curves obtained by the Forbes method are included. The corresponding capillary pressure and average saturation are included (referred to as data).

However, due to the problems encountered with accuracy for the Hassler-Brunner method and the van Domselaar method, the capillary pressure curves obtained by the Forbes method are used for this chalk. Further, Forbes believes this method to produce capillary pressure curves corresponding more closely to the centrifuge data than curves obtained from most other methods. Finally, the Forbes method include constraints. As can be seen from Figure 4.4, 4.5 and 4.6, there is only a small difference between the uncorrected and the corrected Forbes capillary pressure curves for Hillerslev outcrop chalk. However, it is advised (Forbes 1997) always to include the corrections, i.e. account for the radial and gravity effects in order to obtain the most accurate capillary pressure curves

The capillary pressure curves obtained by the corrected Forbes method are reduced by use of the constraints given by Forbes (Section 2.1). The reduced, corrected capillary pressure curves (final capillary pressure curves) are given in Figure 4.7, 4.8 and 4.9 for specimens 1A, 2 and 3, respectively.

The minimum capillary pressure required to force water into specimen 1A was between 0 kPa and 26 kPa, and the minimum capillary pressure required to force oil into the specimen was between 13 kPa and 28 kPa. From the form of the capillary pressure curves, it is evaluated that the obtained end-face residual oil saturation $S_{orw} = 0.34$ is close to the truth whereas S_{wir} is considered to be lower than the obtained end-face water saturation $S_w = 0.03$ due to the centrifuge limitations.

The minimum capillary pressure required to force oil into specimen 2 is between 107 kPa and 137 kPa. Since no water could be forced into specimen 2 after spontaneous imbibition, it is evaluated that the obtained end-face residual oil saturation $S_{orw} = 0.29$ is reliable. The irreducible water saturation S_{wir} is considered to be lower than the obtained

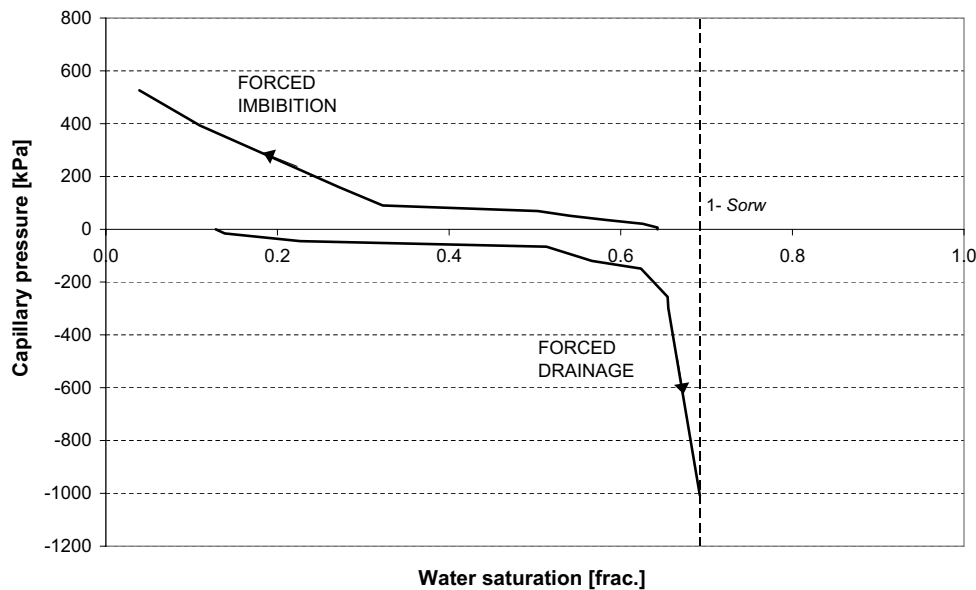


Figure 4.7 Final water-oil capillary pressure curves for specimen 1A.

end-face water saturation $S_w = 0.14$ due to centrifuge limitations.

The minimum capillary pressure required to force oil into specimen 3 is between 137 kPa and 190 kPa. Since no water could be forced into specimen 3 after spontaneous imbibition, it is evaluated that the obtained end-face residual oil saturation $S_{orw} = 0.27$ is reliable. Again, S_{wir} is considered to be lower than the obtained end-face water saturation $S_w = 0.09$ due to centrifuge limitations.

There were no visible fractures before the capillary pressure measurement, but distinct fractures were induced in specimens 1A and 3 during the centrifuging in water. Further, less distinct fractures may have been induced in specimen 2. This changes the fluid flow properties such as permeability of the chalk specimens, and may explain the slight difference in the capillary pressure curves for specimens 2 and 3. This also means that the capillary pressure curves were obtained on slightly fractured specimens.

In centrifuge measurements, sources of error consist of data acquisition and not waiting long enough to obtain a good estimate of equilibrium average saturation at each centrifuge step. At some of the centrifuge steps, hydrostatic equilibrium was defined at too high a production level resulting in too poor data for the capillary pressure curves. Further, interpretation of centrifuge measurement for capillary pressure curves requires a number of assumptions regarding core homogeneity and boundary conditions ($P_c = 0$).

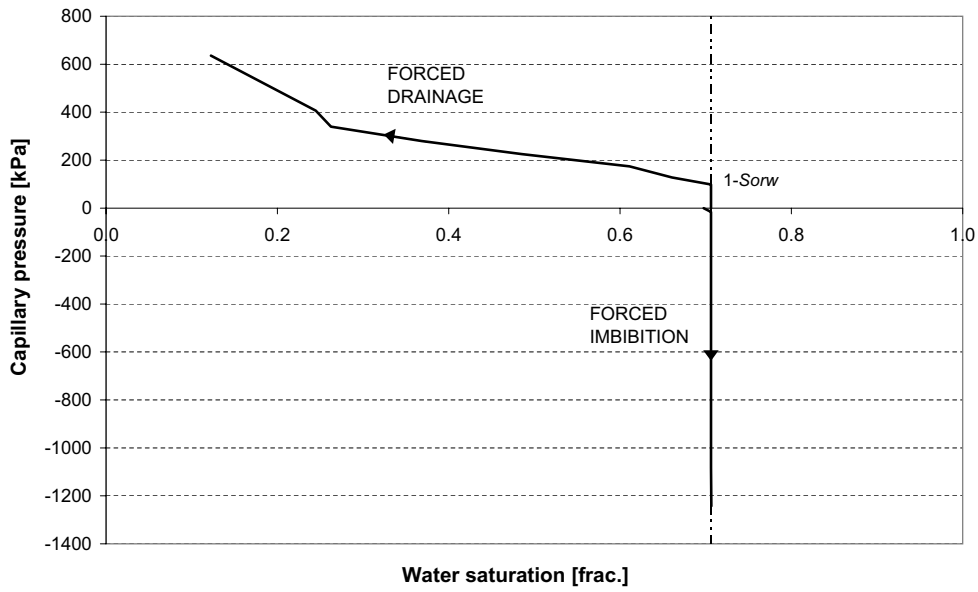


Figure 4.8 Final water-oil capillary pressure curves for specimen 2.

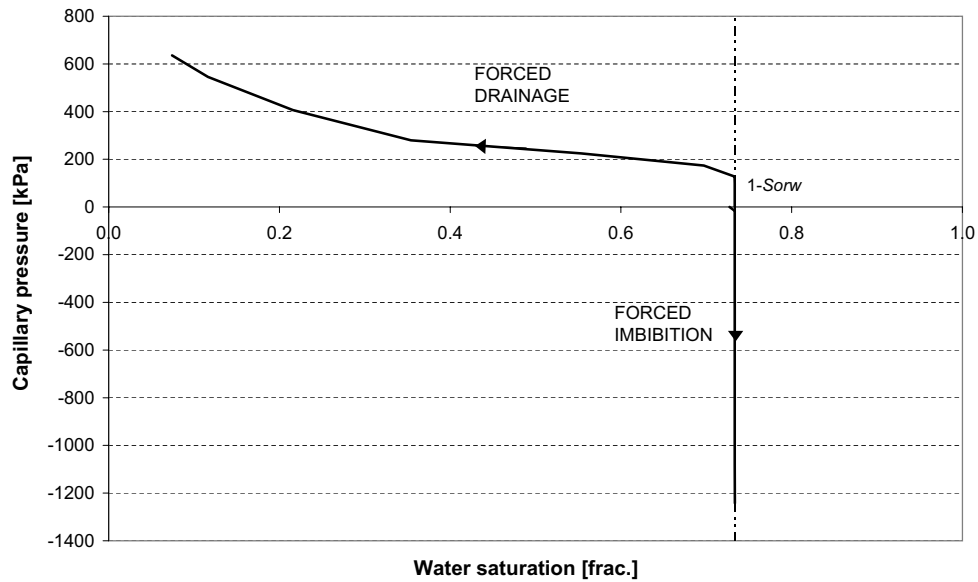


Figure 4.9 Final water-oil capillary pressure curves for specimen 3.

The form of the capillary pressure curves for all three specimens implies that the centrifuge test was ended at too low a capillary pressure. In other words, these capillary pressure curves were not fully completed due to centrifuge speed limitations even though the Beckman centrifuge was run to its maximum capacity of 8000 RPM. This means that the irreducible water saturation S_{wir} was not obtained in any of the specimens at the end of the test.

The form of the capillary pressure curves is affected by the fact that the production at some of the centrifuge steps was not constant at the defined hydrostatic equilibrium. Further, the capillary pressure curves were obtained on slightly fractured specimens. Evaluating this together with the fact that the capillary pressure curves were not fully completed, the obtained capillary pressure curves are not very representative for the three specimens. However, a good estimate of the residual oil saturation S_{orw} is obtained, especially for the strongly water-wet specimens.

The high capillary pressure of chalk makes it difficult to obtain the necessary high rotational speed to establish capillary pressure curves for chalk in the centrifuge. To be able to establish capillary pressure curves for Hillerslev outcrop chalk, a centrifuge of larger capacity must be used. At the same time, the low mechanical strength of chalk implies that the centrifuge speed must be limited to ensure that fractures are not induced in the chalk. Based on this it is evaluated that capillary pressure curves for Hillerslev outcrop chalk cannot be obtained in the centrifuge.

The minimum capillary pressure required to force oil into the strongly water-wet Hillerslev outcrop chalk is so high that the USBM wettability index cannot be obtained. Further, consistent Amott-Harvey and USMB wettability indices cannot be obtained for the wettability altered Hillerslev outcrop chalk specimen using the centrifuge.

This is consistent with the fact that conventional methods used for determination of saturation functions are mainly developed for rocks of lower capillary pressure and higher mechanical strength than chalk. This means that these methods may not apply for chalk. Bech (Bech et al. 2000) states that especially the centrifuge method is unsuitable due to the low mechanical strength of chalk, as well as the difficulty of obtaining the necessary high rotational speed.

Chapter 5

Conclusions

Hillerslev outcrop chalk is described as strongly water-wet. Spontaneous imbibition of water into the strongly water-wet specimens 2 and 3 was in the range of 71-73%. The water imbibed rapidly, and approximately 88% of the spontaneous imbibition was completed within an hour. No water could be forced into specimens 2 and 3 after spontaneous imbibition.

There is no clear evidence of an effect of different initial water saturations S_{wi} on the final average saturation after spontaneous (and forced) water imbibition in strongly water-wet Hillerslev outcrop chalk.

It is concluded that Hillerslev outcrop chalk can be altered towards a homogeneous neutral to slightly oil-wet state using crude oil added with 1 weight% Dodekane acid. However, the alteration affected the chalk as well.

Based on the form of the capillary pressure curves, the fact that the capillary pressure curves were obtained on slightly fractured specimens, and the fact that the capillary pressure curves were not fully completed, it is evaluated that the obtained capillary pressure curves are not fully representative for the three specimens. However, a good estimation of the residual oil saturation S_{orw} is obtained, especially for the strongly water-wet specimens.

Based on the fact that the capillary pressure curves were not fully completed due to centrifuge limitations, and that fractures were induced in the specimens even at these lower centrifuge speeds, it is evaluated that capillary pressure curves for Hillerslev outcrop chalk cannot be obtained in the centrifuge.

The minimum capillary pressure required to force oil into the strongly water-wet Hillerslev outcrop chalk is so high that the USBM wettability index cannot be obtained. Further, consistent Amott-Harvey and USMB wettability indices was not obtained for the wettability altered Hillerslev outcrop chalk specimen using the centrifuge.

Conclusions

Bibliography

- Ali, N. & Alcock, T. (1992), 'Valhall field, norway - the first ten years', *Amoco Norway Oil Co. Norway* .
- Andersen, M. (1995), *Petroleum Research in North Sea Chalk. Joint Chalk Research Phase IV*, Stavanger Research Center.
- Anderson, W. (1986a), 'Wettability literature survey - part 2: Wettability measurement', *SPE* .
- Anderson, W. (1986b), 'Wettability literature survey - part 4: Effects of wettability on capillary pressure', *SPE* .
- Bech, N., Olsen, D. & Nielsen, C. (2000), 'Determination of oil/water saturation functions of chalk core plugs from two-phase flow experiments', *SPE Reservoir Eval. and Eng.* **3(1)**.
- Christensen, H. (2003), Displacement and deformation processes in fractured reservoir chalk, Efp-2000, GEO.
- Christoffersen, K. (1995), 'Gas/oil capillary pressure of chalk at elevated pressures', *SPE Formation Evaluation* .
- Eltvik, P., Skoglunn, T. & Skinnarland, O. (1990), 'Valhall waterflood pilot - a study of water injection in a fractured reservoir', *Proceedings at the Third North Sea Chalk Symposium, Copenhagen, 1990* .
- Forbes, P. (1994), 'Simple and accurate methods for converting centrifuge data into drainage and imbibition capillary pressure curves', *The Log Analyst* .
- Forbes, P. (1997), 'Quantitative evaluation and correction of gravity effects on centrifuge capillary pressure curves', *Society of Core Analysts* (SCA-9734).
- Hassler, G. & Brunner, E. (1945), 'Measurements of capillary pressure in small core samples', *Transactions AIME* **160**, 114–123.
- Jakobsen, F. (2001), Fractures and rock mechanics. phase 2. description of natural and test induced fractures in chalk, EFP-98 Report 2001/18, GEUS.
- Krogsbøll, A., Jakobsen, F. & Madsen, L. (1997), Fractures and rock mechanics. phase 1. geology report, EFP-96 Report 1997/63, GEUS.

Bibliography

- Man, H. & Jing, X. (2000), 'Network modelling of mixed-wettability on electrical resistivity. capillary pressure and wettability indices', *6th International Symposium on Evaluation of Reservoir Wettability and Its Effect on Oil Recovery*. Socorro. New Mexico. USA .
- Morrow, N. (1990), 'Wettability and its effect on oil recovery', *JPT* .
- Nørgaard, J., Olsen, D., Reffstrup, J. & Springer, N. (1999), 'Capillary pressure curves for low permeability chalk obtained by nuclear magnetic resonance imaging of core saturation profiles', *SPE Reservoir Evaluation and Engineering* 2,2 pp. 141–148.
- Pub (1983), *Beckman Instruments. Instructions for using the Type PIR 16.5 Rotor in the Beckman Model L5-50P Ultracentrifuge*.
- Ruth, D. & Chen, Z. (1995), 'Measurement and interpretation of centrifuge capillary pressure curves - the sca survey data', *The Log Analyst* .
- Skauge, A. & Poulsen, S. (2000), 'Rate effects on centrifuge drainage relative permeability', *Soc. Petr. Eng.* (SPE 63145).
- Szabo, M. (1974), 'New methods for measuring imbibition capillary pressure and electrical resistivity curves by centrifuge', *Society of Petroleum Engineers Journal* pp. 243–252.
- Verbruggen, M., Farmer, R. & Adams, S. (2000), 'State-of-the-art scal experiments and interpretation', *Proceedings at New Zealand Petroleum Conference, 19-22 March 2000* .

Appendix A

Discrete Solutions for End-Face Saturation

Discrete solutions to the fundamental saturation equation for converting average specimen saturation into end-face saturation.

Drainage

The solution to the fundamental saturation equation for drainage can be evaluated with high accuracy from discrete \bar{S} data using a simple differencing scheme (Forbes 1994):

$$S_{i-1/2+B/4} \approx S_{\alpha\beta i-1/2+B/4} = \left(1 - \frac{B}{2}\right) S_{\alpha i-1/2} + \frac{B}{2} S_{\beta i} \quad (\text{A.1})$$

$$B = 1 - \left(\frac{r_1}{r_3}\right)^2 \quad 0 \leq B \leq 1 \quad (\text{A.2})$$

$$\alpha = \frac{1 - \sqrt{1-B}}{1 + 2\sqrt{1-B}} = \frac{r_3 - r_1}{r_3 + 2r_1} \quad (\text{A.3})$$

$$\beta = \frac{2}{\alpha} \quad (\text{A.4})$$

$$S_{\alpha i-1/2} = \frac{\bar{S}_i - \left(\frac{P_{i-1}}{P_i}\right)^{1+\alpha} \bar{S}_{i-1}}{1 - \left(\frac{P_{i-1}}{P_i}\right)^{1+\alpha}} \quad (\text{A.5})$$

$$S_{\beta i} = \left(\frac{P_{i-1}}{P_i}\right)^{1+\beta} S_{\beta i-1} + \frac{1 - \left(\frac{P_{i-1}}{P_i}\right)^{1+\beta}}{1 - \left(\frac{P_{i-1}}{P_i}\right)} \left(\bar{S}_i - \left(\frac{P_{i-1}}{P_i}\right) \bar{S}_{i-1}\right) \quad (\text{A.6})$$

Using this scheme, solution S for step i is obtained directly from the values of \bar{S} at steps i and $i-1$ and from the value of S at step $i-1$. No iteration, smoothing, fitting, numerical integration or specific numerical treatment are needed.

Imbibition

The solution to the fundamental saturation equation for imbibition can be evaluated with high accuracy from discrete \bar{S} data using a simple differencing scheme (Forbes 1994):

$$S_{i-1/2} \approx S_{\alpha i-1/2} = \frac{\bar{S}_i - \left(\frac{P_{i-1}}{P_i}\right)^{1+\alpha} \bar{S}_{i-1}}{1 - \left(\frac{P_{i-1}}{P_i}\right)^{1+\alpha}} \quad (\text{A.7})$$

$$B = 1 - \left(\frac{r_3}{r_1}\right)^2 \quad B < 0 \quad (\text{A.8})$$

$$\alpha = \frac{1 - \sqrt{1-B}}{1 + 2\sqrt{1-B}} = \frac{r_3 - r_1}{r_3 + 2r_1} \quad (\text{A.9})$$

Using this scheme, solution S for step i is obtained directly from the values of \bar{S} at steps i and $i-1$ and from the value of S at step $i-1$. No iteration, smoothing, fitting, numerical integration or specific numerical treatment are needed.

Appendix B

Gravity and Radial Effects on Capillary Pressure

When rotating, the fluids in the specimen are subjected to the centrifugal field, $1/2\rho\omega^2r^2$, and to the gravity field, $-\rho gZ$, where ρ is the fluid density, g is the gravitational acceleration, ω is the angular velocity and (r, Z) refer to the cylindrical coordinates. At hydrostatic equilibrium, the pressure is (Ruth & Chen 1995):

$$P = \frac{1}{2}\rho\omega^2r^2 - \rho gZ + Const. \quad (\text{B.1})$$

The capillary pressure is then given by:

$$P_c(r, Z, \omega) = -\frac{1}{2}\Delta\rho\omega^2r^2 + \Delta\rho gZ + Cons. \quad (\text{B.2})$$

The value of the constant "Const." is obtained from the boundary condition hypothesis, i.e. that $P_c = 0$, where the inner fluid is flowing out of the specimen.

By definition, the average saturation of the specimen \bar{S} is:

$$\bar{S} = \frac{1}{L\pi R^2} \int_{specimen} S_{r,Z,\omega} dv = \frac{1}{L\pi R^2} \int_{specimen} S(P_c(r, Z, \omega)) r dr d\theta dZ \quad (\text{B.3})$$

where L is the length of the core, R is the radius of the core, r the rotational radius, Z is the vertical coordinate and dv is the elementary volume.

Drainage

For a cylindrical specimen in a drainage experiment: $P_c = 0$ is located at the border of the circular outflow face of the specimen, the face furthest from the axis of rotation, for $Z = -R$, if $g/\omega^2 > R$ or, for $Z = -g/\omega^2$, if $g/\omega^2 < R$, leading to:

$$P_c(r, Z, \omega) = \frac{1}{2}\Delta\rho\omega^2(r_3^2 - r^2) + \Delta\rho gZ + \frac{1}{2}\Delta\rho\omega^2(n+1)R^2 \quad (\text{B.4})$$

where $n = 2(g/\omega^2)/R - 1$ if $g/\omega^2 > R$, or $n = (g/\omega^2)^2/R^2$ if $g/\omega^2 < R$.

$P_c(r, Z, \omega)$ varies inside the specimen, and the above equation can be normalized and re-written as:

$$\bar{S}_{B,N,M} = \frac{1 + \sqrt{1-B}}{2} \int_{x=0}^{x=1} \frac{dx}{\sqrt{1-Bx}} \int_{y=0}^{y=1} \frac{2}{\pi} \sqrt{\frac{y}{1-y}} dy \int_{z=0}^{z=1} \frac{1}{2} S(P_1(x+Ny+2NMz\sqrt{y}+Nn)) dz \quad (\text{B.5})$$

using the normalized parameters:

$$\begin{aligned} B &= 1 - \left(\frac{r_1}{r_3}\right)^2 \\ N &= \frac{R^2}{r_3^2 - r_1^2} \\ M &= \frac{g}{\omega^2 R} \\ P_1 &= \frac{1}{2} \Delta\rho\omega^2 (r_3^2 - r_1^2) \end{aligned}$$

and the normalized variables:

$$\begin{aligned} x &= \frac{1 - \left(\frac{r}{r_3}\right)^2 (\cos\theta)^2}{B} \\ y &= 1 - \frac{\left(\frac{r}{r_3}\right)^2 (\sin\theta)^2}{NB} \\ z &= Z/R/\sqrt{y} \end{aligned}$$

Imbibition

For a cylindrical specimen in an imbibition experiment: $P_c = 0$ is located on the top of the outflow face of the specimen, the face nearest from the axis of rotation, and:

$$P_c(r, Z, \omega) = \frac{1}{2} \Delta\rho\omega^2 (r_1^2 - r^2) + \Delta\rho g Z + \frac{1}{2} \Delta\rho\omega^2 (n+1) R^2 \quad (\text{B.6})$$

with $n = -2(g/\omega^2)/R - 1$.

$P_c(r, Z, \omega)$ varies inside the specimen, and the above equation can be normalized and re-written as:

$$\bar{S}_{B,N,M} = \frac{1 + \sqrt{1-B}}{2} \int_{x=0}^{x=1} \frac{dx}{\sqrt{1-Bx}} \int_{y=0}^{y=1} \frac{2}{\pi} \sqrt{\frac{y}{1-y}} dy \int_{z=-1}^{z=1} \frac{1}{2} S(P_3(x+Ny+2NMz\sqrt{y}+Nn)) dz \quad (\text{B.7})$$

using the normalized parameters:

$$\begin{aligned} B &= 1 - \left(\frac{r_3}{r_1}\right)^2 \\ N &= \frac{R^2}{r_1^2 - r_3^2} \\ M &= -\frac{g}{\omega^2 R} \\ P_3 &= \frac{1}{2} \Delta\rho\omega^2 (r_1^2 - r_3^2) \end{aligned}$$

and the normalized variables:

$$\begin{aligned}x &= \frac{1 - \left(\frac{r}{r_1}\right)^2 (\cos \theta)^2}{B} \\y &= 1 - \frac{\left(\frac{r}{r_1}\right)^2 (\sin \theta)^2}{NB} \\x &= Z/R/\sqrt{y}\end{aligned}$$

Appendix C

Laboratory Journal

25/04/01	Two specimens (S1 & S2) were drilled from a chalk block. S1 & S2 were drilled with a $\phi 42$ drill cooled with water. S1 & S2 were placed in an oven at 105°C overnight for drying.
26/04/01	S1 & S2 were turned in a turning lathe to a diameter of 38 mm and then cut by an electric saw at both ends to a length of 50 mm. S1 & S2 were described, sketched and photographed.
27/04/01	S1 & S2 were placed in an oven at 105°C over the weekend for drying.
30/04/01	Mixing of formation water (brine) after Valhall field recipe. A shrink fix sleeve was put around each specimen. S1 & S2 were weighed, and placed in Exxon Triaxial core holders. Isopar-H was injected into the core holders via a pump to ensure a pressure around the cores (overburden pressure). This pressure was chosen to 20 bar. S1 & S2 were then saturated with brine by applying vacuum. The brine-saturated S1 & S2 were removed from the core holders and weighed. S1 & S2 were placed in the core holders with an overburden pressure of 20 bar.
01/05/01	Rate test with brine for determination of the absolute (brine) permeability for S1 & S2. Mean brine permeabilities of 2.9 mD and 2.6 mD for specimen 1 and 2, respectively.
09/05/01	Displacement of brine by Isopar-L to S_{wi} in S1 & S2 by use of a pump. First displacement of brine by Isopar-L until breakthrough and then displacement by Marcol (displacement of Isopar-L and brine). The high viscosity Marcol is used to obtain as low S_{wi} as possible.
14/05/01	One specimen (S3) was drilled from a chalk block. S3 was drilled with a $\phi 42$ drill cooled with water. S3 was placed in an oven at 105°C for drying.
15/05/01	S3 was turned in a turning lathe to a diameter of 38 mm and then cut by an electric saw at both ends to a length of 50 mm. S3 was described, sketched and photographed. S3 was placed in an oven at 105°C for drying.
18/05/01	A shrink fix sleeve was put on the specimen. S3 was weighed, and placed in Exxon Triaxial core holder. Isopar-H was injected into the core holder via a pump to ensure a 20 bar pressure around the core (overburden pressure). S3 was then saturated with Isopar-L by applying vacuum. The Isopar-L-saturated S3 was weighed, and placed in the core holder again with an overburden pressure of 20 bar.
19/05/01	Displacement of Marcol by Isopar-L in S1 & S2. Total production of brine S1: 21.95 cm^3 & S2: 18.53 cm^3 .
21/05/01	Displacement of Isopar-L by Snorre oil added 1 weight% Dodekane acid in S1. Flushing with 100 ml in each direction. S1 was placed in a piston cell at 8 bar and 90°C for aging
25/06/01	Aging of S1 was ended. S2 & S3 were taken out of the core holders and placed in cups with

	Isopar-L. S1 was removed from the piston cell, and broke in one end. S1 was placed in core holder again with 20 bar overburden pressure. Snorre oil displaced by Isopar-L at 40°C in S1.
27/06/01	S1 removed from core holder after displacement by Isopar-L. S1 now slightly uneven and greyish S1 was cut by an electric saw at both ends to a length of 36.2 mm. S1 was cut in both ends to reduce capillary end effect. S1, S2 & S3 were placed in Amott cups with brine for spontaneous production of Isopar-L. Within 1.5 hour the imbibition was almost completed.
28/06/01	Spontaneous displacement completed. S1: no Isopar-L production, S2: 10.8 cm ³ & S3: 19.3 cm ³ . S1, S2 & S3 were removed from the Amott cups and placed in inverted Beckman centrifuge buckets with brine for forced production of Isopar-L. Centrifuge test initiated.
15/07/01	Centrifuge test ended at maximum capacity of the centrifuge, i.e. 7700 RPM. S1: 9.20 cm ³ , S2 & S3 no production of Isopar-L. S1, S2 & S3 were placed in Amott cups with Isopar-L for spontaneous production of brine.
-	Spontaneous displacement completed. S1: 0.12 cm ³ , S2 & S3: no brine production. S1, S2 & S3 were removed from the Amott cups and placed in standard Beckman centrifuge buckets with Isopar-L for forced production of brine. Centrifuge test initiated.
12/09/01	Centrifuge test ended at maximum capacity of the centrifuge, i.e. 8000 RPM. S1: 7.80 cm ³ , S2: 11.09 cm ³ & S3: 12.06 cm ³ .

Table C.1: Laboratory journal for specimens 1, 2 and 3.

Appendix D

Description of Specimens 1, 2 and 3

Specimen 1

Specimen 1 is very light grey with areas of a darker grey colour (clay). Small inhomogeneities were seen in the surface of the specimen due to the turning in a turning lathe. A rust-coloured area was seen. A small piece of flint was observed. A sketch of specimen 1 is seen in Figure D.1.

A mean diameter of $D = 3.81$ cm and a mean height of $H = 5.00$ cm was measured.

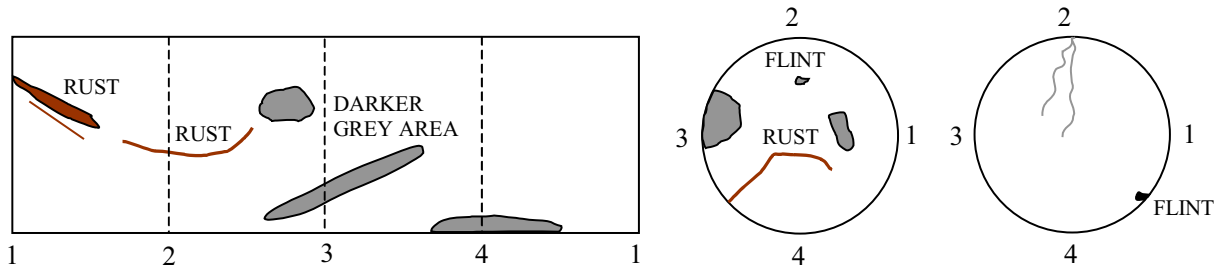


Figure D.1 *Sketch of specimen 1.*

The specimen broke in one end when removed from the cell after aging in Snorre oil added 1 weight% Dodekane acid ($C_{11}H_{23}COOH$). The specimen was cut in both ends partly to even the broken surface and partly to reduce capillary end effect in the unbroken end, where approximately 2 mm was cut off. The specimen is now referred to as specimen 1A. A new mean height was measured to $H = 3.62$ cm.

The displacement of Snorre oil with Isopar-L caused the periphery of the specimen to become uneven. Under the assumption that porosity, dry density and fluid saturations were unchanged, the mean diameter was calculated to $D = 3.79$ cm.

Specimen 2

Specimen 2 is very light grey with many areas of a darker grey colour (clay). Small inhomogeneities were seen in the surface of the specimen due to the turning in a turning lathe. Flint was observed. A sketch of specimen 2 is seen in Figure D.2.

Description of Specimens 1, 2 and 3

A mean diameter of $D = 3.80$ cm and a new mean height of $H = 5.00$ cm was measured.

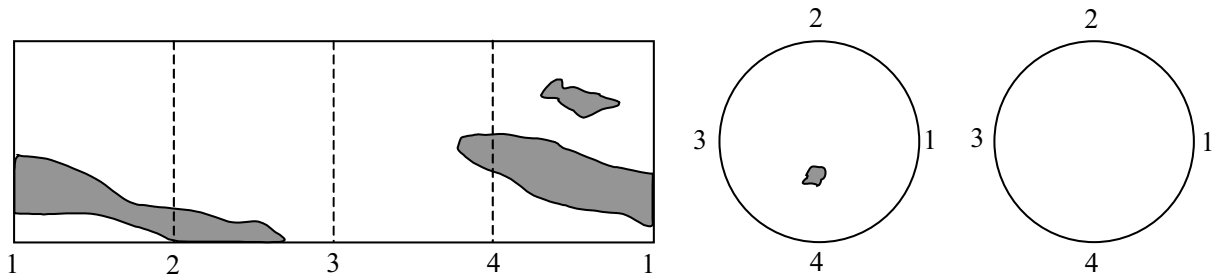


Figure D.2 *Sketch of specimen 2.*

Specimen 3

Specimen 3 is very light grey with few very small areas of a darker grey colour (clay). Small inhomogenities were seen in the surface of the specimen due to the turning in a turning lathe. A sketch of specimen 3 is seen in Figure D.3.

A mean diameter of $D = 3.81$ cm and a mean height of $H = 5.00$ cm was measured.

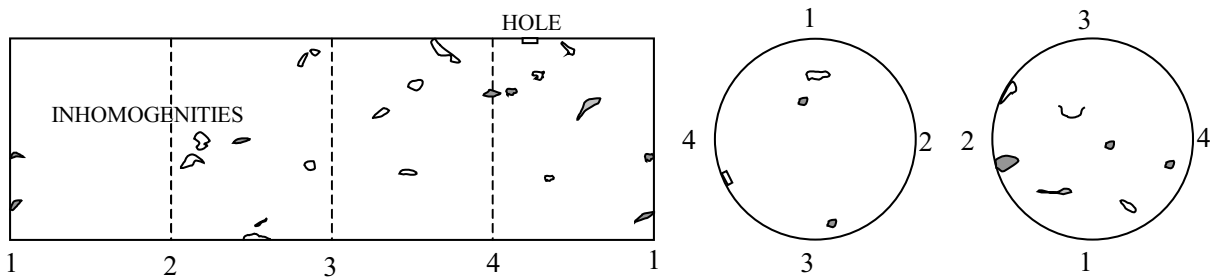


Figure D.3 *Sketch of specimen 3.*

Appendix E

Absolute Water Permeability for Specimens 1 and 2

Permeability is a measure of the ability of the porous medium to conduct one or more fluids. Provided that the porous medium is completely saturated with one fluid, the absolute, intrinsic permeability K [m^2] ($1 \text{ D} = 9.869 \cdot 10^{-13} \text{m}^2$) of the medium is determined as:

$$K = \frac{Q\mu L}{A\Delta P} \quad (\text{E.1})$$

where Q [m^3/s] is the volumetric flow rate, μ [Pas] is the viscosity of the fluid, L [m] is the actual length of the specimen, A [m^2] is the cross sectional area of the specimen and ΔP [Pa] is the differential pressure over the specimen.

Corresponding values of flow and pressure difference were measured to determine the absolute water permeability of the fully water saturated specimens (specimens 1 and 2). The fluid used was synthetic Valhall formation water referred to here as water. The measurements were performed at a backpressure of 3 bar. The test set-up is shown in Figure 3.2.

Mean absolute water permeabilities for specimens 1 and 2 are 2.9 mD and 2.6 mD, respectively.

Absolute Water Permeability for Specimens 1 and 2

Q [$\cdot 10^{-6} \text{m}^3/\text{s}$]	ΔP [kPa]	K [mD]
0.0017	26.20	2.83
0.0025	32.75	3.39
0.0033	51.50	2.88
0.0042	63.57	2.91
0.0050	74.88	2.97
0.0058	88.87	2.92
0.0050	76.26	2.91
0.0042	63.71	2.91
0.0033	51.50	2.88
0.0017	26.37	2.81
0.0013	19.79	2.81

Table E.1 *Absolute water permeability for specimen 1.*

Q [$\cdot 10^{-6} \text{m}^3/\text{s}$]	ΔP [kPa]	K [mD]
0.0050	82.19	2.72
0.0042	69.15	2.69
0.0033	55.50	2.68
0.0025	41.85	2.67
0.0017	29.03	2.56
0.0008	15.48	2.40

Table E.2 *Absolute water permeability for specimen 2.*

Appendix F

Production Curves for the Centrifuge Tests

Production Curves for the Centrifuge Tests

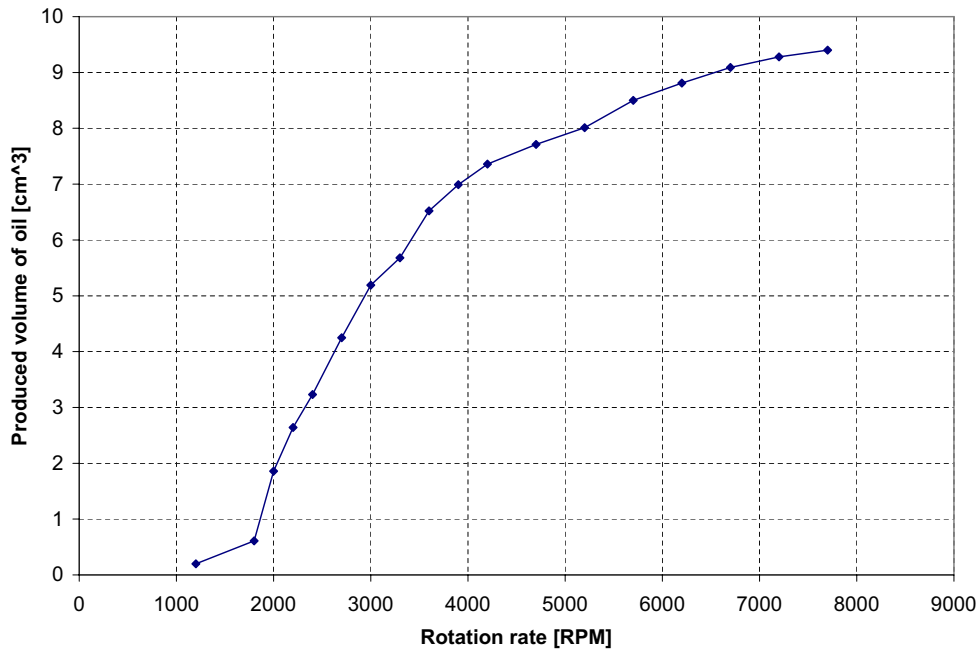


Figure F.1 Production of oil vs. rotation rate for specimen 1A. Total oil production of 9.20 cm^3 from the pore volume of 19.12 cm^3 .

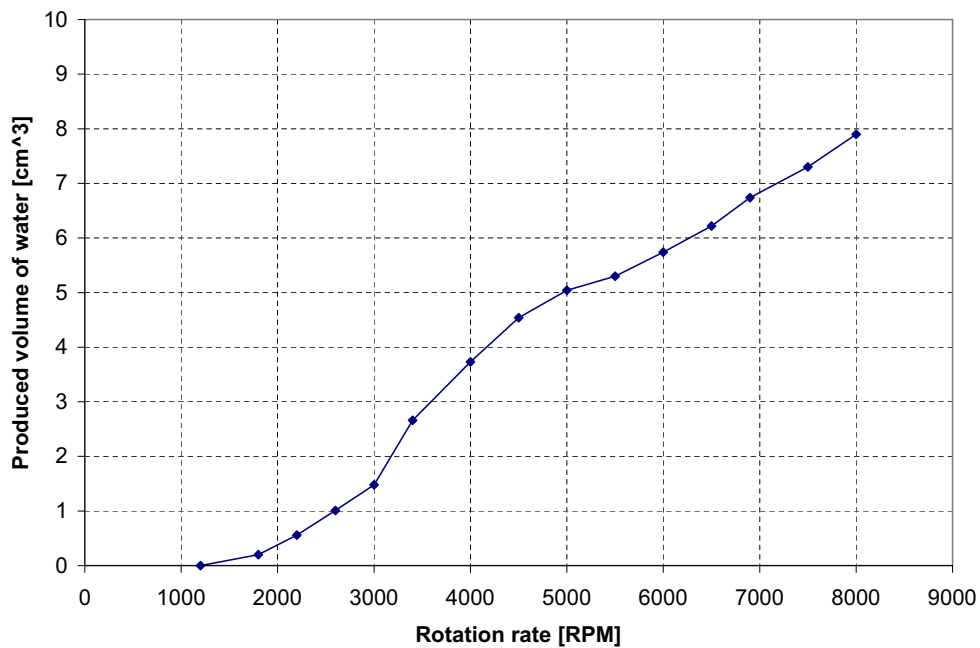


Figure F.2 Production of water vs. rotation rate for specimen 1A. Total water production of 7.80 cm^3 from the pore volume of 19.12 cm^3 .

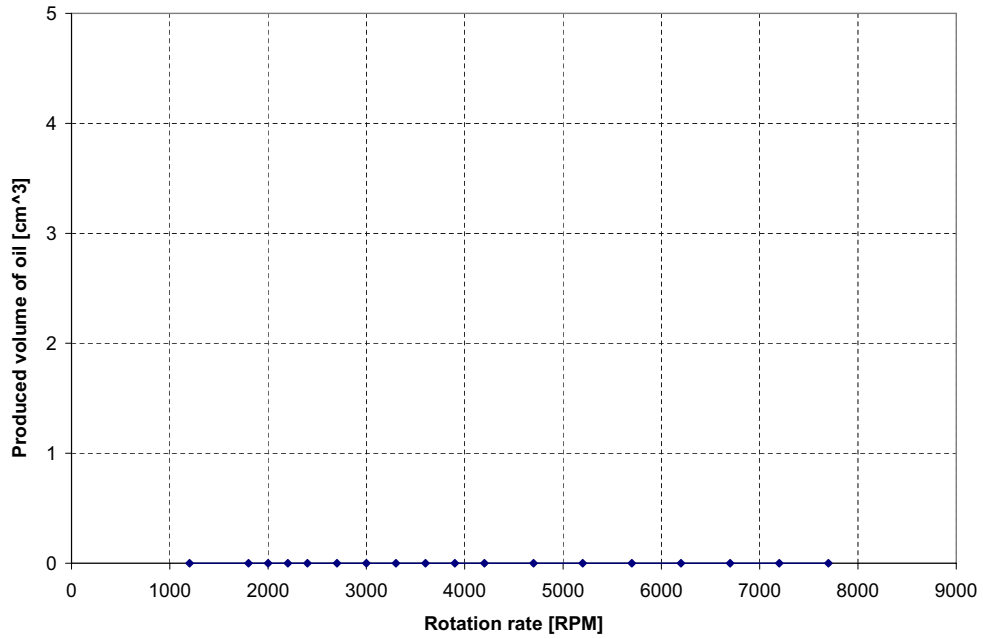


Figure F.3 Production of oil vs. rotation rate for specimen 2. No oil production.

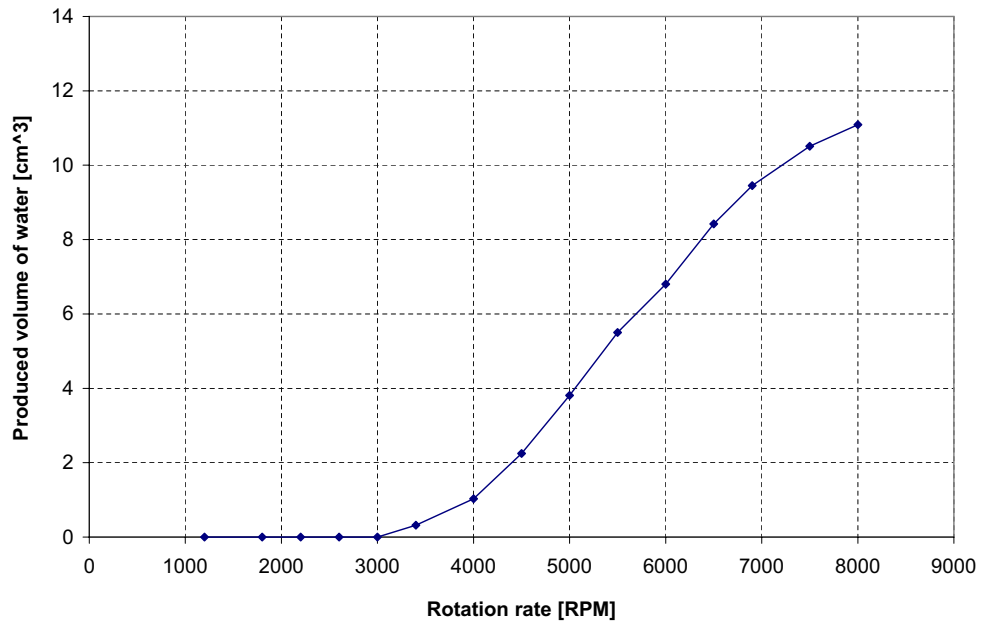


Figure F.4 Production of water vs. rotation rate for specimen 2. Total water production of 11.09 cm³ from the pore volume of 26.55 cm³.

Production Curves for the Centrifuge Tests

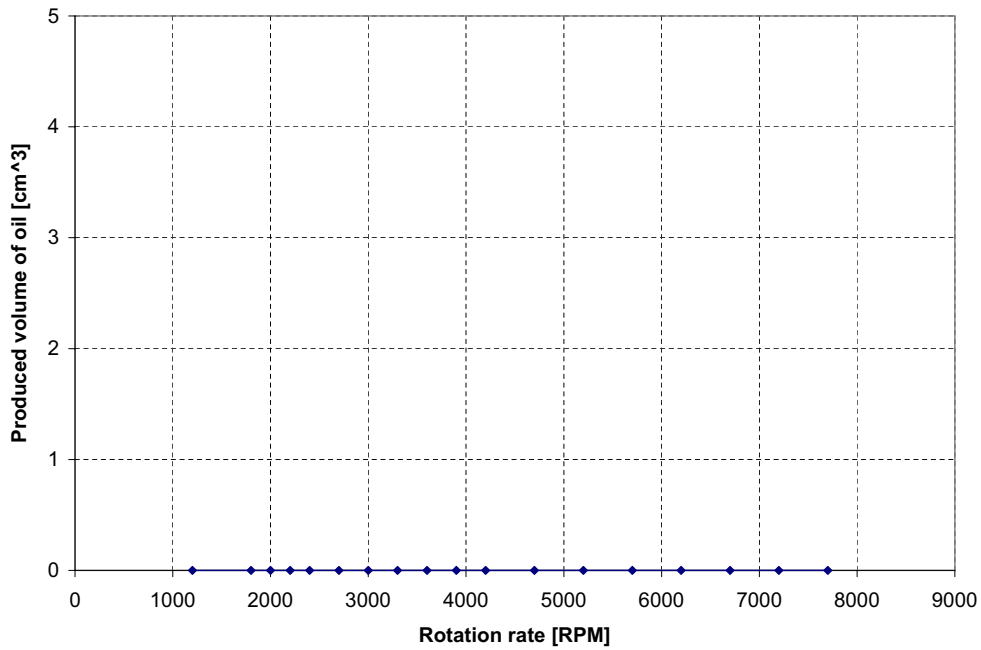


Figure F.5 Production of oil vs. rotation rate for specimen 3. No oil production.

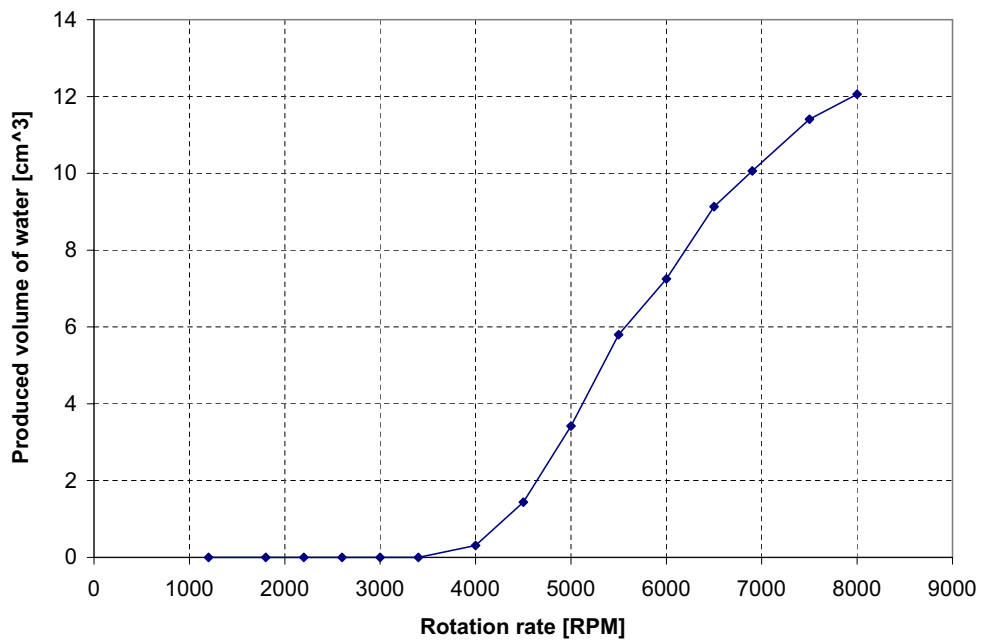


Figure F.6 Production of water vs. rotation rate for specimen 3. Total water production of 12.06 cm³ from the pore volume of 26.84 cm³.